AD NUMBER

AD823517

LIMITATION CHANGES

TO:

Approved for public release; distribution is unlimited.

FROM:

Distribution authorized to U.S. Gov't. agencies and their contractors; Critical Technology; OCT 1967. Other requests shall be referred to Air Force Technical Application Center, Washington, DC 20333. This document contains export-controlled technical data.

AUTHORITY

usaf ltr, 25 jun 1972

LARGE-ARRAY SIGNAL AND NOISE ANALYSIS

Special Scientific Report No. 13

SHORT-PERIOD NOISE COHERENCE AMONG SUBARRAYS

Prepared by

Frank H. Binder, Program Manager

TEXAS INSTRUMENTS INCORPORATED
Science Services Division
P. O. Box 5621
Dallas, Texas 75222

Contract No. AF 33(657)-16678

Prepared for

AIR FORCE TECHNICAL APPLICATIONS CENTER
Washington, D. C. 20333

Sponsored by

ADVANCED RESEARCH PROJECTS AGENCY
ARPA Order No. 599
AFTAC Project No. VT/6707

20 October 1967

LARGE-ARRAY SIGNAL AND NOISE ANALYSIS

Special Scientific Report No. 13

SHORT-PERIOD NOISE COHERENCE AMONG SUBARRAYS

Prepared by

Frank H. Binder, Program Manager

TEXAS INSTRUMENTS INCORPORATED
Science Services Division
P. O. Box 5621
Dallas, Texas 75222

Contract No. AF 33(657)-16678

Prepared for

AIR FORCE TECHNICAL APPLICATIONS CENTER
Washington, D. C. 20333

Sponsored by

ADVANCED RESEARCH PROJECTS AGENCY
ARPA Order No. 599
AFTAC Project No. VT/6707

20 October 1967

TABLE OF CONTENTS

LIST OF TABLES

LIST OF ILLUSTRATIONS

LIST OF ILLUSTRATIONS (CONTD)

SECTION I
INTRODUCTION AND SUMMARY

Much of the analysis of the mantle P-wave noise proposed for this contract depended on the ability to treat the LASA as a large array, i.e., to perform coherent processing by treating seismic noise as a compilation of plane waves using the large aperture available at LASA. The subarray outputs should be P-wave-limited, and the large array could be used to dissect the P-wave noise; therefore, it is extremely important to understand the coherence of the subarray outputs.

Considerable effort has been expended to determine coherence among subarray outputs. This report presents the results of coherence studies among subarrays.

The principal results of the study are

- Development of a program to compute multiple coherences and thus estimate multichannel coherence
- Development and programing of a new processing technique to design filters that maximize the coherence between the output of two groups of sensors (group coherence)
- Presentation of results of measured 2-channel and multiple coherence, indicating that the subarray outputs generally are moderately coherent below about 1 cps only within the B ring of the subarrays

- Presentation of 2-channel and multiple coherences for several possible noise models. A study of these coherences suggests that the most reasonable models would give little coherence between A0 and the E and F rings. Comparison of model-study results with measured coherences suggests that a considerable portion (25 percent or more) of the sub-array output power is not interpretable as seismic energy

SECTION II
DISCUSSION OF COHERENCE

Coherence is a measure of the predictability of the primary channel from the other channels as a function of frequency. Consider a least-mean-square prediction of one channel from n-1 others in the frequency domain. The correlation matrix formed from the variables is a crosspower matrix which can be partitioned as follows:

$$\begin{vmatrix} \Phi_{11} & \Omega_{12} \\ \Omega_{21} & \Omega_{22} \end{vmatrix}$$

where

Φ_{11} is the autopower of the trace being predicted

Ω_{12} is the row vector of crosspowers Φ_{12} through Φ_{1n}

Ω_{21} is Ω_{12}^{*}

Ω_{22} is the crosspower matrix formed by channels 2 through n

The solution is filter weights of $\Omega_{12}\,\Omega_{22}^{-1}$ and prediction-error variance (autopower) of $\Phi_{11} - \Omega_{12}\,\Omega_{22}^{-1}\,\Omega_{21}$ or

$$\Phi_{11}\left(1 - \frac{\Omega_{12}\,\Omega_{22}^{-1}\,\Omega_{21}}{\Phi_{11}}\right)$$

Coherence, as used in this report, is defined as

$$\frac{\Omega_{12}\,\Omega_{22}^{-1}\,\Omega_{21}}{\Phi_{11}}$$

For the 2-channel case, this reduced to

$$\frac{\Phi_{12}\;\Phi_{21}}{\Phi_{11}\;\Phi_{22}}$$

Thus, (1 - coherence), whether 2-channel or multiple coherence, can be interpreted as the fraction of the power in the primary trace which cannot be predicted from the other traces. True coherence is unchanged by the application of linear filtering to any or all traces.

Coherence is a random variable which must be estimated. Estimation of coherence is determined from the estimation of the cross-power matrix. The crosspower matrix is estimated by some scheme from a finite data sample and may not accurately reflect the ensemble statistics. The result may be an overestimate or an underestimate of coherence.

Schemes to estimate power spectra involve smoothing (in the frequency domain) to give the estimate stability. This smoothing introduces a bias into the crosspower spectral estimates, making them systematically low. Smoothing does not bias the autopower estimates and thus makes the expected values of the coherence estimates too low. This can be a severe problem when there is considerable time delay among channels.

For example, consider two channels which are exactly the same except that one is delayed by τ:

$$f_1(t) = f(t)$$

$$f_2(t) = f(t+\tau)$$

Assume that the traces are sampled at an interval of ΔT and that the samples have a total length $N\Delta T$. Let $\tau = K\Delta T$. If the crosspower matrix is to be estimated by direct transform methods, the data are transformed according to the dictates of the sampling theorem ($\Delta f = 1/N\Delta T$) and the crosspower estimate is of the form

$$\frac{1}{C} \sum_{M=\alpha}^{\alpha+C-1} F_1^{*}(M\Delta f)\, F_2(M\Delta f)$$

where

$\Delta f = 1/N\Delta T$

C = number of frequency points in smoothing interval

$F_1(f)$ = discrete Fourier transform of $f_1(t)$

$F_2(f)$ = discrete Fourier transform of $f_2(t)$

The crosspower at each frequency ($f = M\Delta f$) will be

$$\exp\left[2\pi i f\tau\right] = \exp\left[2\pi i \frac{M}{N\Delta T} K\Delta T\right] = \exp\left[2\pi i \frac{MK}{N}\right]$$

For notational compactness, let K/N = Q. Therefore, the estimate of the crosspower becomes

$$\frac{1}{C}\sum_{M=\alpha}^{\alpha+C-1} \exp(2\pi i MQ) = \frac{\exp(2\pi i \alpha Q)\left[\exp(2\pi i CQ) - 1\right]}{C\left[\exp(2\pi i Q) - 1\right]}$$

$$= \frac{\sin \pi CQ}{C \sin \pi Q} \exp\left[2\pi i Q\left(\alpha + \frac{C}{2} - \frac{1}{2}\right)\right]$$

Thus, the crosspower estimate is reduced by a factor $(\sin \pi CQ / C \sin \pi Q)$.

Consider an example which would be reasonable for two LASA subarrays (A0 and C ring) with 100-point smoothing. For a noise sample dominated by a 10-km/sec plane wave, $K \approx 20$, $N \approx 4000$, $Q \approx 1/200$, and $C = 100$; then, the coherence would be reduced by about 1/1.57.

This biasing effect makes the estimation of crosspowers between the widely spaced LASA subarrays very difficult. Extremely long noise samples would be necessary to estimate adequately a crosspower spectrum from two positions approximately 100-km apart.

SECTION III

MULTIPLE-COHERENCE PROGRAM

A rigorous mathematical derivation of the multiple coherence (R^2) for weakly stationary Gaussian processes has been given by L. H. Koopmans.[1] The calculation is based on the fact that a crosspower matrix is a covariance matrix of random variables, which is the Fourier transform of a sample of time-series data. Since Fourier transforms are linear combinations of multivariate normal data, they also are distributed multivariate normal. One then uses the body of theorems about conditional distributions for multivariate normal data. The actual calculations are done iteratively (over an increasing number of sensors), using the exact equations given by Koopmans.[1]

An entirely analogous development of the equations for calculating multiple correlations, which is mathematically much easier to handle rigorously, is given by T. W. Anderson.[2] This method of estimating multichannel coherence or predictability is computationally very rapid compared to the design of prediction filters and the evaluation of their performance. The method is especially useful when several different combinations of sensors are desired.

The program estimates the crosspower spectra by taking the direct transform of time-series data, using the Cooley-Tukey algorithm, and setting $\Phi_{ij}(f) = F_i^*(f)\, F_j(f)$. Stability is obtained by averaging adjacent frequencies. The distribution of the estimate of the multiple coherence ($\bar{R}^2$) has been derived by N. R. Goodman[3] under the assumption that the frequency vectors (direct transforms of time-series data) used in the averaging are independent. This leads to density function

$$p(\bar{R}^2) = \frac{\Gamma(n)}{\Gamma(p-1)\,\Gamma(n-p+1)} (1-R^2)(\bar{R}^2)^{p-2}(1-\bar{R}^2)^{n-p} F(n,n;p-1;R^2\,\bar{R}^2)$$

where

$\overline{R}^2$ is the multiple coherence estimate

R^2 is the true population multiple coherence

Γ is the gamma function

F is the hypergeometric function

p is the number of channels

n is the number of frequencies used in the formation of the crosspower matrix estimate

This reduces to a Beta distribution when the data are uncorrelated ($R^2 = 0$).

In estimating the multiple coherences, 80-point (0.2-cps) smoothing with 4096 (409.6-sec) noise samples generally were used. Table III-1 gives the mean for $R^2 = 0$, n = 80, and p = 1 through 15.

Table III-1

MEAN VALUE OF MULTIPLE-COHERENCE ESTIMATE

p	Mean
1	1/82 = 0.012195
2	2/82 = 0.024390
3	3/82 = 0.036585
4	4/82 = 0.048780
5	5/82 = 0.060976
6	6/82 = 0.073171
7	7/82 = 0.085366
8	8/82 = 0.097561
9	9/82 = 0.109756
10	10/82 = 0.121951
11	11/82 = 0.134146
12	12/82 = 0.146341
13	13/82 = 0.158537
14	14/82 = 0.170732
15	15/82 = 0.182927

Burg[4] has shown that the ratio of the mean-square-error for an estimated filter to the mean-square-error for the true ensemble filter in a prediction problem is independent of the data's covariance matrix.

$(1 - \overline{R}^2)$ can be interpreted as the fraction of prediction-error power. This is not exactly the form required by Burg's theorem (fractional as opposed to true prediction-error power) but, if the data sample is assumed to give an accurate spectral estimate of the primary trace (the one to be predicted), the results can be extrapolated to correlated noise. If the mean value of multiple coherence for the uncorrelated data were 0.15, then, from [0.85 (MSE in prediction estimated)/1.0(MSE for ensemble average)], one would expect a noise sample with 0.98 true multiple coherence to give an estimate $(\overline{R}^2/0.02) \approx 0.85$. Thus $1 - \overline{R}^2 = (0.02)(0.85) = 0.017$.

This analysis is not rigorous but does indicate that the estimated multiple coherence becomes much more reliable (in terms of absolute error) as the true coherence increases.

SECTION IV

2-CHANNEL COHERENCES

To get an initial idea of the coherence among subarrays, outputs of the MCF system were used to calculate 2-channel coherences between the A0 and the B1, B2, B3, C1, C2, C3, C4, D1, D2, D3, and D4 subarrays. (Figure IV-1 shows the large-array configuration.) This was done for an 8-min noise sample recorded 25 March 1966 from 04:18 to 04:26. Data were prewhitened, using a single deconvolution filter, before the coherences shown in Figure IV-2 were computed.

These coherences are probably not meaningful at very low frequencies ($f < 0.1$ cps), because nonseismic noise likely makes up a considerable portion of the power at these low frequencies. The short-period seismometer response is such that low-frequency ground motion is severely attenuated.

The 2-channel coherences have the following salient features:

- They fall off sharply with increasing distance; there is almost no coherence between A0 and subarrays of the D ring
- All closer subarrays (within 13 km) except C4 show a peak coherence near 1/3 cps, which is near the microseism peak; Figure IV-3 shows the power spectrum of the MCF output for subarray A0, and this low-frequency coherence is very likely caused by the directional surface-mode energy

Theoretical coherences generated by some plausible theoretical noise models in $f\text{-}\vec{k}$ space were computed. These models are generated from combinations of the $|\text{crosspowers}|^2$ which results from disk or annulus distribution of power in the K plane (at a fixed frequency).

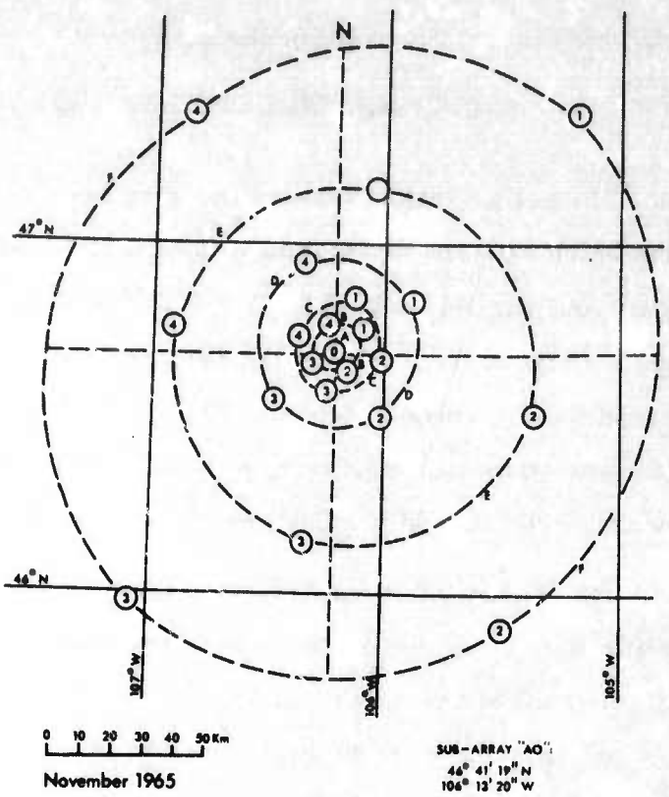

LASA

NAME	AZIMUTH	DELTA-KM	THETA	X	Y
B1	54.902	12.312	35.098	10.07330	7.07912
B2	141.477	7.614	308.523	4.74223	-5.95686
B3	246.010	8.039	203.990	-7.34456	-3.26849
B4	347.011	9.063	102.989	-2.03704	8.83111
C1	23.531	18.291	66.469	7.30259	16.77000
C2	97.459	16.245	352.541	16.10754	-2.10883
C3	191.498	12.981	258.502	-2.58753	-12.72050
C4	294.023	12.769	155.977	-11.66298	5.19829
D1	56.459	30.497	33.541	25.41896	16.85062
D2	141.708	26.250	308.292	16.26637	-20.60261
D3	232.156	25.110	217.844	-19.82894	-15.40536
D4	336.360	30.753	113.640	-12.33163	28.17229
E1	13.507	54.221	76.493	12.66405	52.72133
E2	106.254	68.551	343.746	65.81109	-19.18699
E3	188.314	60.556	261.686	-8.75616	-59.91960
E4	278.849	53.706	171.151	-53.06676	8.26157
F1	45.670	109.262	44.330	78.15803	76.35121
F2	146.491	103.543	303.509	57.16296	-86.33393
F3	220.066	103.487	229.934	-66.61130	-79.19908
F4	325.943	97.244	124.057	-54.45840	80.56474

Figure IV-1. Layout of LASA

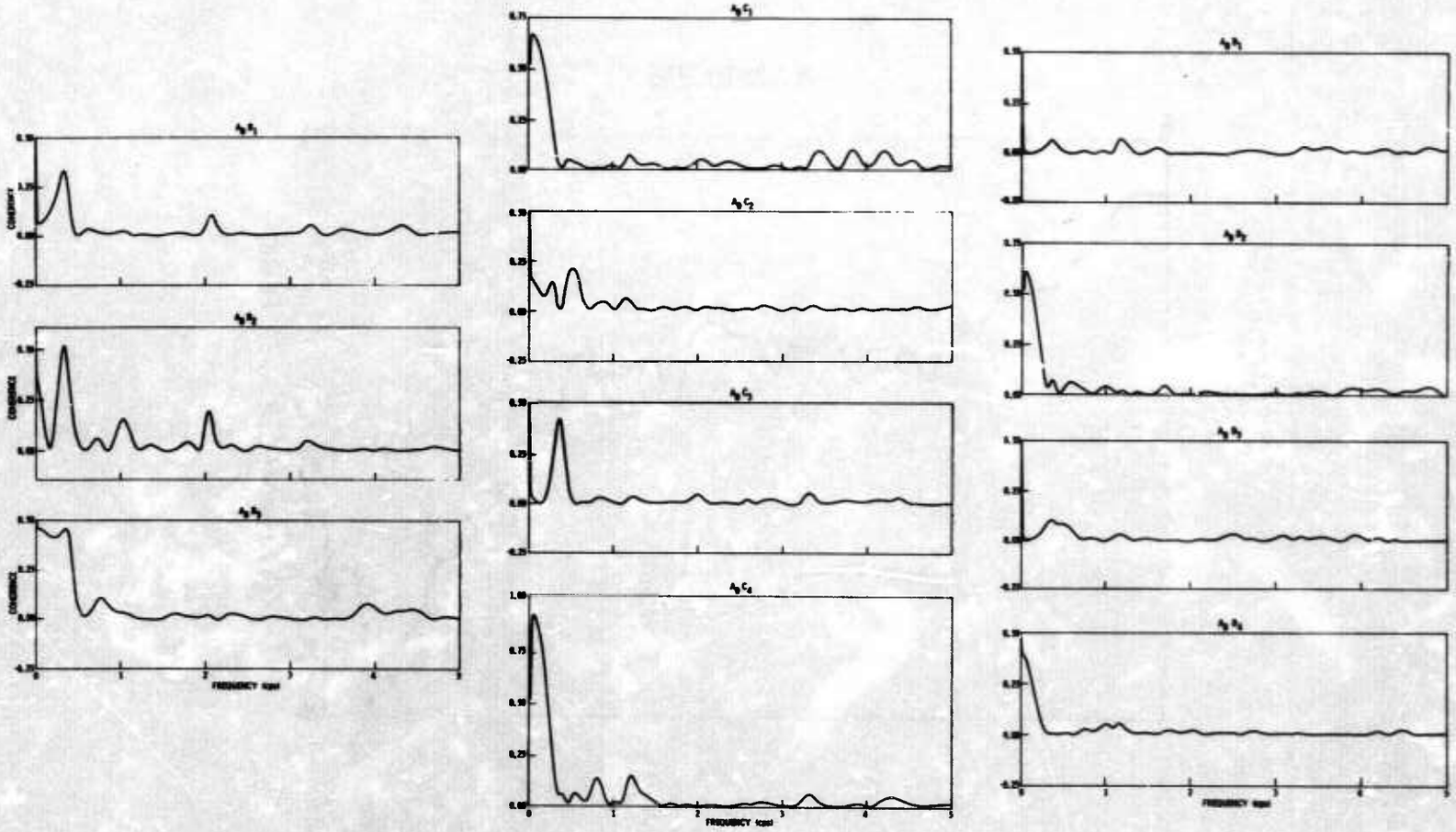

Figure IV-2. 2-Channel Coherences for 25 March 1966 Noise Sample

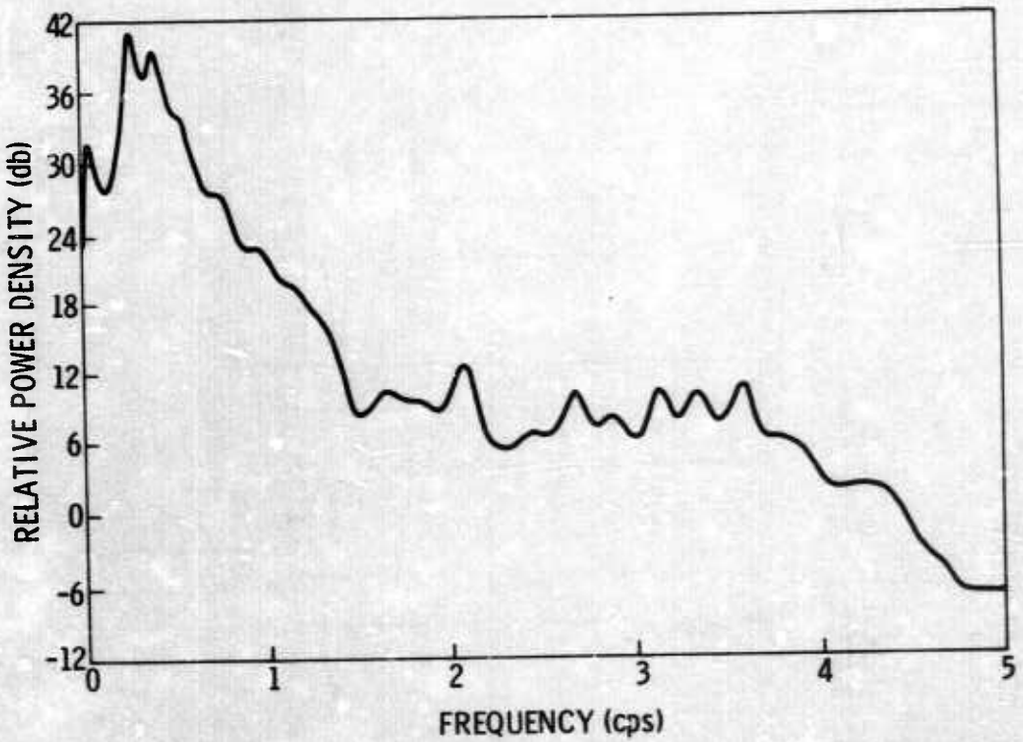

Figure IV-3. Power Spectra of MCF Output Subarray A0, 25 March 1960

The formulas for the disk and annulus are as follows:

Disk:
$$\Phi_{12}(f) = \frac{V_e}{\pi f |X|} J_1 \frac{(2\pi f |X|)}{V_e}$$

where

V_e = lower velocity or radius of the disk (km/sec)

f = frequency (cps)

X = separation of seismometers (km)

Annulus:
$$\Phi_{12}(f) = \frac{1}{\pi f |X| \left[\frac{1}{V_e^2} - \frac{1}{V_u^2}\right]} \left[\frac{1}{V_e} J_1 \left(\frac{2\pi f |X|}{V_e}\right) - \frac{1}{V_u} J_1 \left(\frac{2\pi f |X|}{V_u}\right)\right]$$

where

V_e = velocity of outside radius of annulus

V_u = velocity of inside radius of annulus

J_1 = 1^{st}-order Bessel function

For shifted disk, the crosspower from a centered disk is modified by multiplying the formula for the centered disk by

$$\exp\left[i\,2\pi \left|\left(\frac{\vec{f}}{V}\right)\right| |\vec{X}| \cos \psi\right]$$

where

$\left(\frac{\vec{f}}{V}\right)$ is the vector location (in the K plane) of the center of the disk

$\vec{X}$ is the vector separation of the seismometers

ψ is the angle between $\vec{K}$ and $\vec{X}$

Figure IV-4 (a, b, c) shows the plots calculated for three different disks in the K plane. The model used was a disk of uniform power density out to wavenumbers corresponding to the velocities shown. The horizontal scale is $f|X|$, allowing the frequency to be scaled according to the sensor separation desired. Thus, for a 10-km separation, the horizontal scale would be interpreted as ranging from 0 to 2.6 cps in frequency.

Figure IV-4 shows the coherence obtained from an annular noise model. The noise was assumed to be uniformly distributed in an annulus between V = 10 km/sec and V = 20 km/sec.

Figures IV-4e and IV-4f show the coherences obtained from a model made up of two and three shifted disks, respectively. These disks were designed to correspond to a circular region in the K plane, which would fit precisely into an annulus of 12 km/sec to 18 km/sec. This is equivalent (in size) to a disk centered at K = 0 (V = ∞) with a minimum velocity of 72 km/sec. The center of these shifted disks is a V = 14.4 km/sec.

For models involving shifted disks, coherences are a function of the relative orientation of the noise power model and the sensor locations. For the 2-disk model, the disks and the sensor are centered on the X axis. For the 3-disk model, the disks are separated by 120°, with one disk centered on the K_X axis and the sensors placed on the X axis.

The models are all based on various concepts of the distribution of the mantle P-wave noise.

The two larger disks (V_e = 8 km/sec and V_e = 12 km/sec) treat the P-wave energy as isotropic. For large sensor separations ($|X|$ > 10 km/sec), these models would give essentially no coherence except at low frequencies (f < 0.5 cps).

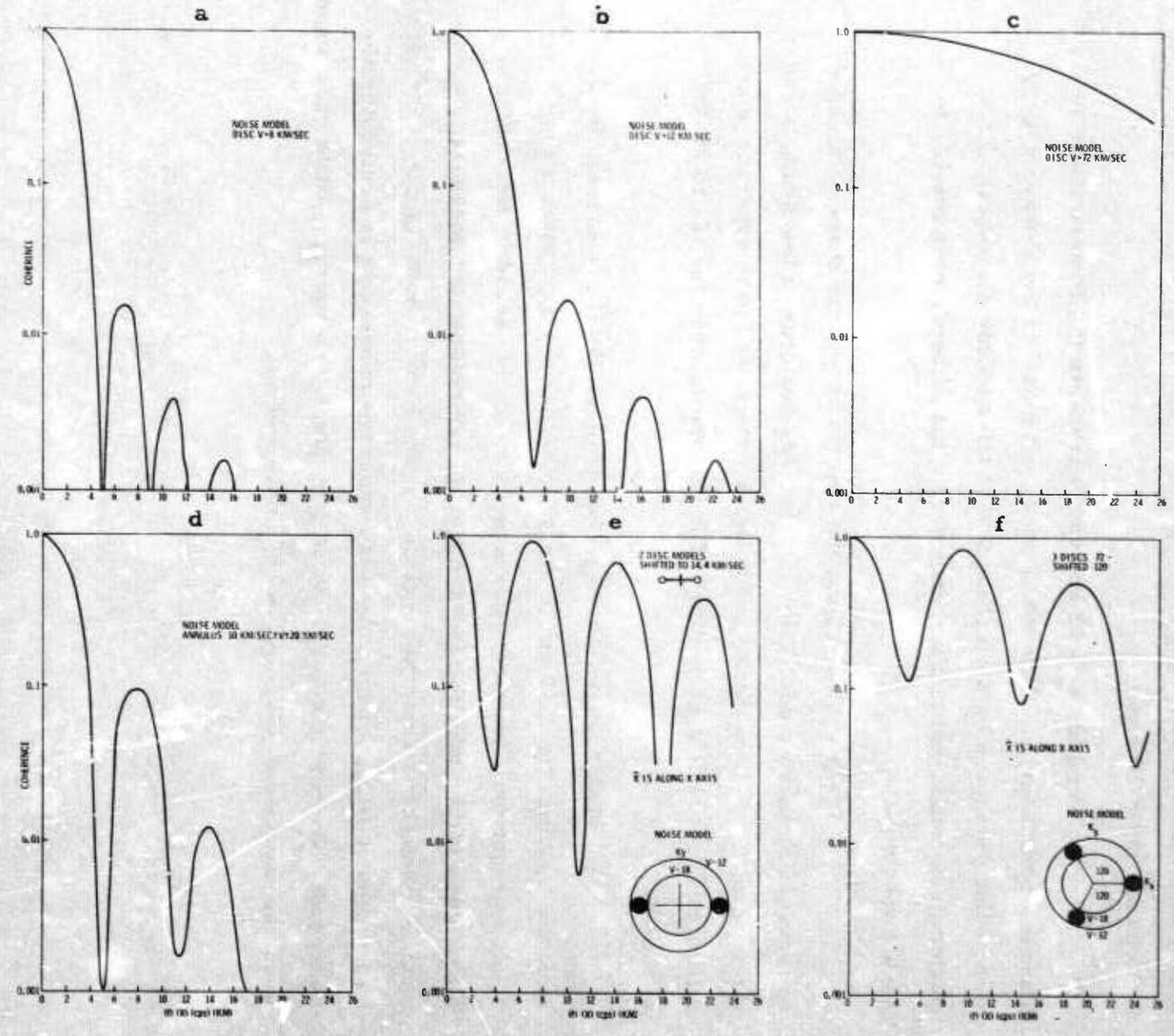

Figure IV-4. 2-Channel Coherences from Theoretical Models

The 10- to 20-km/sec annulus model approximately represents a model of P-wave noise which is uniformly generated from teleseismic distances to the core shadow region. Again, there is little coherence above 0.3 cps for $|X| > 10$ km.

The disk $V_e = 72$ km/sec represents the P-wave noise as almost a point source. This would be a good model if the P-wave energy were being generated by a single storm at teleseismic distances. This model gives considerable coherence over a broad band, even for 10- to 20-km spacings.

Figure IV-4c shows the results of two and three point-like sources. For these models, the interference patterns of the sources cause the coherences to have peaks and nulls; however, the peak coherences are still significant over a good range of frequencies, even for 10- to 20-km spacings.

The 2-channel coherences (Figure IV-1) are essentially 0, even for spacings near 10 km (B ring), except at the microseism peak. The coherence near the microseism pieak is likely caused by the surface-mode noise rather than the P-wave noise. Therefore, the measured 2-channel coherences seem to preclude that the P-wave noise is due essentially to a few point-like sources unless the subarray processing is destroying the coherence. Even with noise dominated by point-like sources, little coherence would be expected at large distances (50 to 100 km).

SECTION V

MULTICHANNEL COHERENCE OF LASA NOISE

Multichannel coherence of subarray outputs was studied for the noise samples given in Table V-1. To calculate multiple coherences between A0 and subarrays through the D ring for these noise samples, the time traces were filled out to 4096 points by adding 0's and estimating the crosspower matrix from the direct transform method using the Cooley-Tukey algorithm. In all cases, the smoothing was 0.2 cps, or about 80 frequency points ($\Delta f = 1/(n\Delta t) = 1/409.6$ cps).

Table V-1

NOISE SAMPLES

Date	Approximate Starting Time	No. Points Used ($\Delta t = 0.1$ sec)
29 October 1965	21:01	3400
4 November 1965	00:42	2950
10 November 1965	02:00	3300
25 November 1965	03:40	2048
4 December 1965	03:07	3400
21 December 1965	08:41	3490
21 January 1966	06:57	4096
5 February 1966	03:02	4096
25 March 1966	04:34	4096
8 April 1966	05:02	4096
15 April 1966	06:44	4096
29 April 1966	09:34	4096

As indicated in Section II, such smoothing can severely reduce the coherence when the separation of sensors is fairly large (D ring or greater). This effect should be reduced somewhat by considering the multiple coherences by rings. Some sensors on the D ring should be located in such a way that they have relatively little moveout with respect to A0.

Also calculated were the multiple correlations from several reasonable models in the f-$\vec{k}$ space of the mantle P-wave noise. These are presented for their intrinsic interest and as a basis for interpreting the observed multichannel coherences.

The noise sample recorded on 25 March 1966 served as the pilot test for the multichannel coherence studies and, therefore, was processed more intensively. Using this 4800-point 8-min noise sample, the following multichannel filter systems were designed:

- A filter to predict A0 MCF output from B1, B2, B3, C2, C3, C4, D1, D2, D3, and D4 MCF outputs
- A filter to predict A0 Σ output from B1, B2, B3, C2, C3, C4, D1, D2, D3, and D4 Σ outputs
- A filter to predict A0 Z-21 output from B1, B2, B3, C2, C3, C4, D1, D2, D3, and D4 Z-21 outputs
- A filter to predict A0 MCF output from C2, C3, C4, D1, D2, D3, and D4 MCF outputs
- A filter to predict A0 MCF output from D1, D2, D3, and D4 MCF outputs

All of the above filters were designed in the time domain from prewhitened data and were 41 points (4.1 sec) long.

Figure V-1 shows the fractional prediction error as a function of frequency in predicting the A0 output using subarrays B1, B2, B3, C2, C3, C4, D1, D2, D3, and D4 where -3 db corresponds to 50-percent predictability and -6 db corresponds to 75-percent predictability. These curves are calculated by taking the ratio of the power spectrum of the prediction error to the power spectrum of the reference trace.

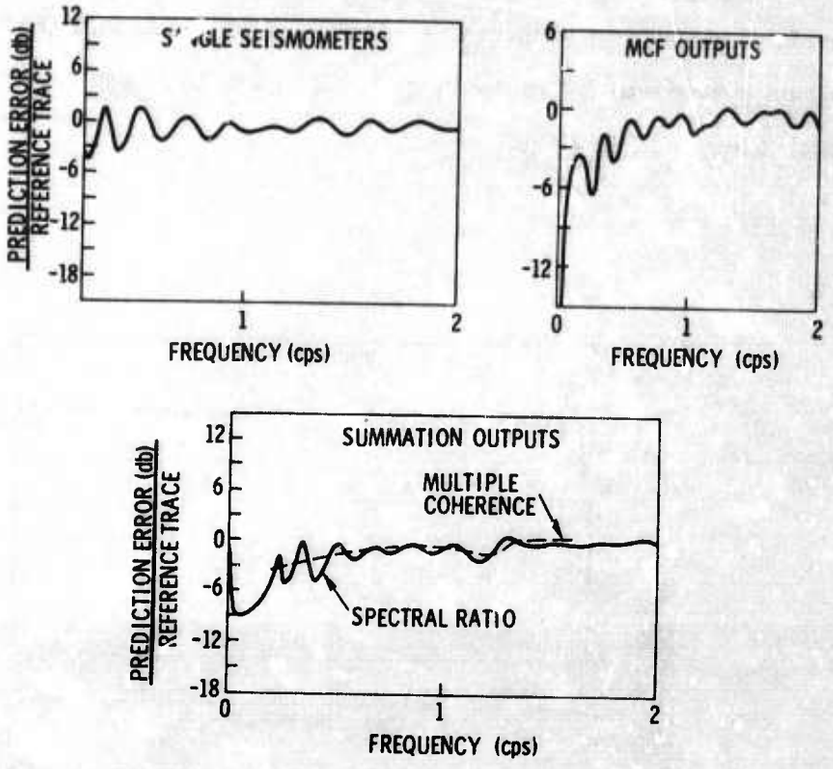

Figure V-1. Prediction Error for 25 March 1966 Noise Sample (B, C, D Rings)

This noise is most predictable near the microseism peak and appears to be moderately predictable below 0.5 cps. Between 0.5 and 1.25 cps, the noise is slightly predictable; from 0 to about 30 percent of the power is predictable. Above 1.25 cps, the noise is generally unpredictable.

Summation and MCF outputs give comparable predictability, while single seismometer outputs are somewhat less predictable.

Superimposed on Figure V-1 (bottom graph) is the prediction error given by the multiple coherence; 4096 points are used and the smoothing interval is 0.25 cps, giving approximately 100 points in the frequency domain. There is general agreement between the two different methods.

Figure V-2 shows the fractional prediction error obtained using the MCF outputs of subarrays composed of the C and D rings and of the D ring only to predict the A0 output. Results indicate that the predictability comes from the B and C rings.

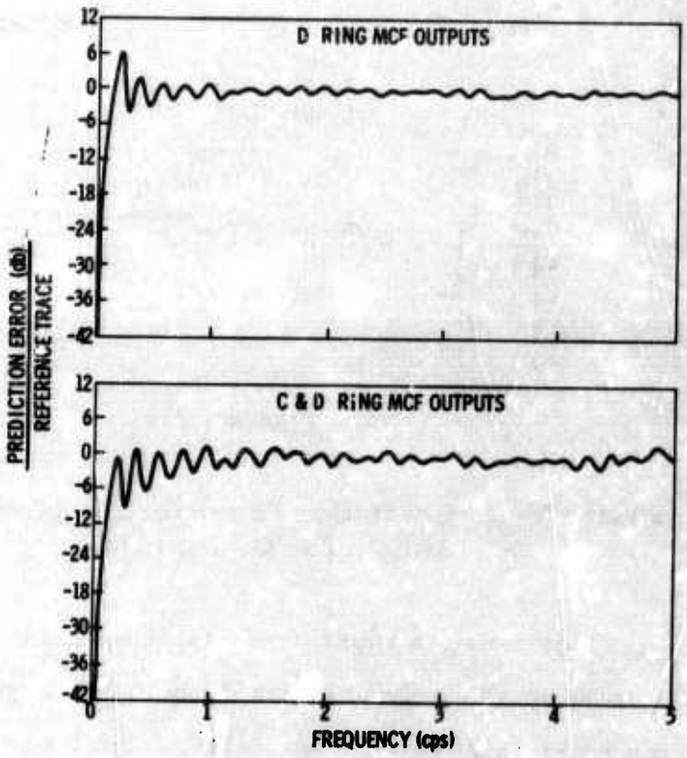

Figure V-2. Prediction Error for 25 March 1966 Noise Sample (C and D Rings)

Figures V-3 through V-14 show the calculated multiple coherence of subarray MCF outputs for the 12 noise samples listed in Table V-1. These figures show the prediction error (E) as a function of frequency when using different combinations to predict the A0 output. The subarray outputs used to predict A0 in each plot are identified above each plot. In general, the noise shows little coherence outside the B ring. Coherences between A0 and the C and D rings are generally almost 0 or small; however, the 15 April 1966 noise sample (Figure V-13) is an exception.

Maximum coherences between A0 and the subarrays included in the B ring are usually about 0.75; 75 percent of the power in A0 output is predictable. The maximum coherence occurs near the microseism peak and is very likely influenced by surface-mode noise which is "getting through" the subarray velocity filtering.

In general, it appears that coherence attributable to the mantle P-wave noise exists only within the B ring and at frequencies below 0.8 cps. This coherence is generally 0.25 to 0.70 in this interval.

Several noise samples show coherent peaks at higher frequencies ($1.5 < f < 2.0$ cps), which are very likely the result of locally generated noise.

The 15 April 1966 noise sample (Figure V-13) appears to be anomalous. While the low frequency ($f < 0.8$ cps) portion of this sample appears to have characteristics similar to the other noise samples, a quite coherent peak occurs at approximately 1.0 to 1.2 cps. The 15 April 1966 noise sample is unique in that a point-like source of high-velocity noise is present near 1.0 cps. This source constitutes about 80 percent of the total power. Characteristics of this noise sample are discussed in more detail in another report.[4]

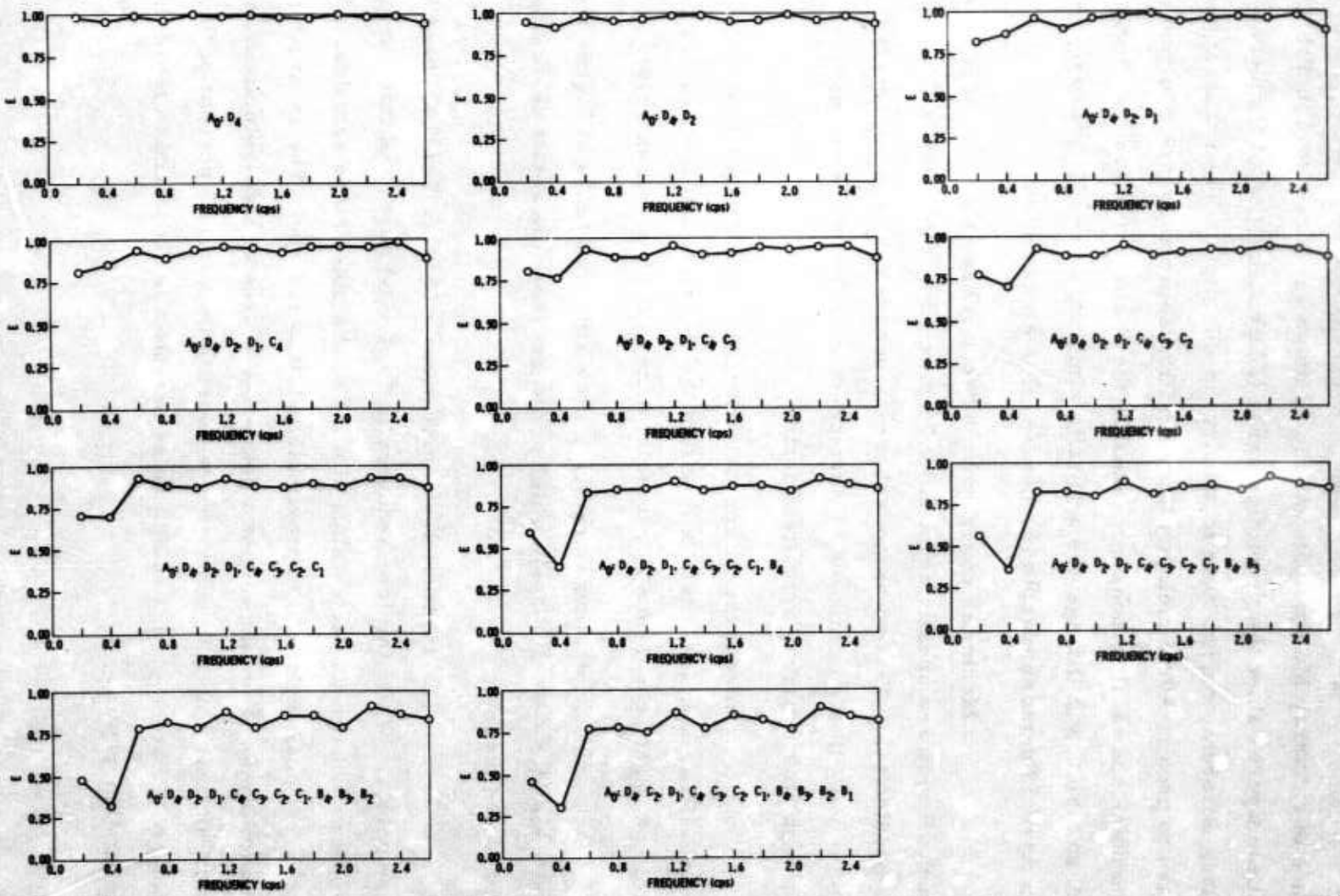

Figure V-3. Multiple Coherences, 29 October 1965

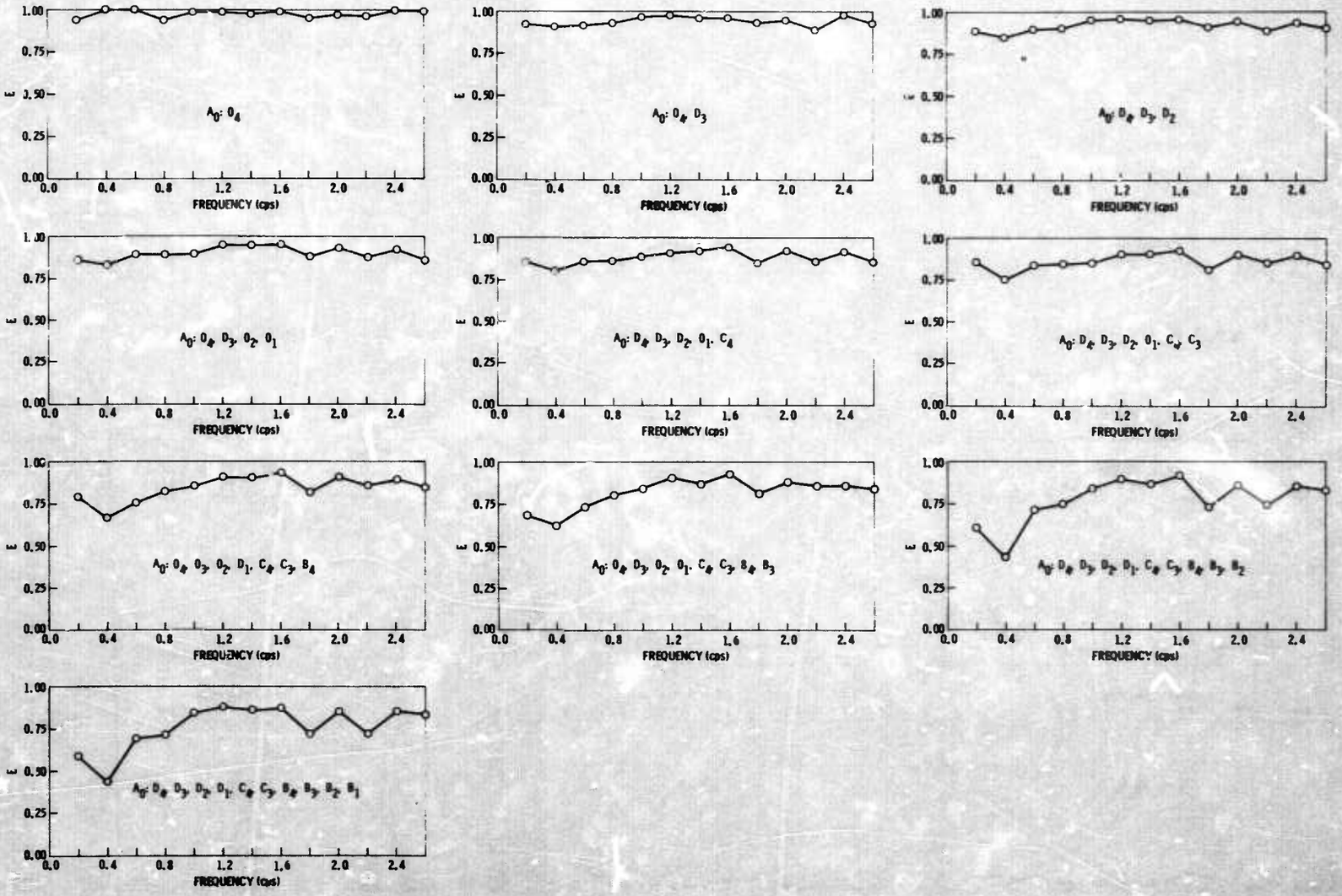

Figure V-4. Multiple Coherences, 4 November 1965

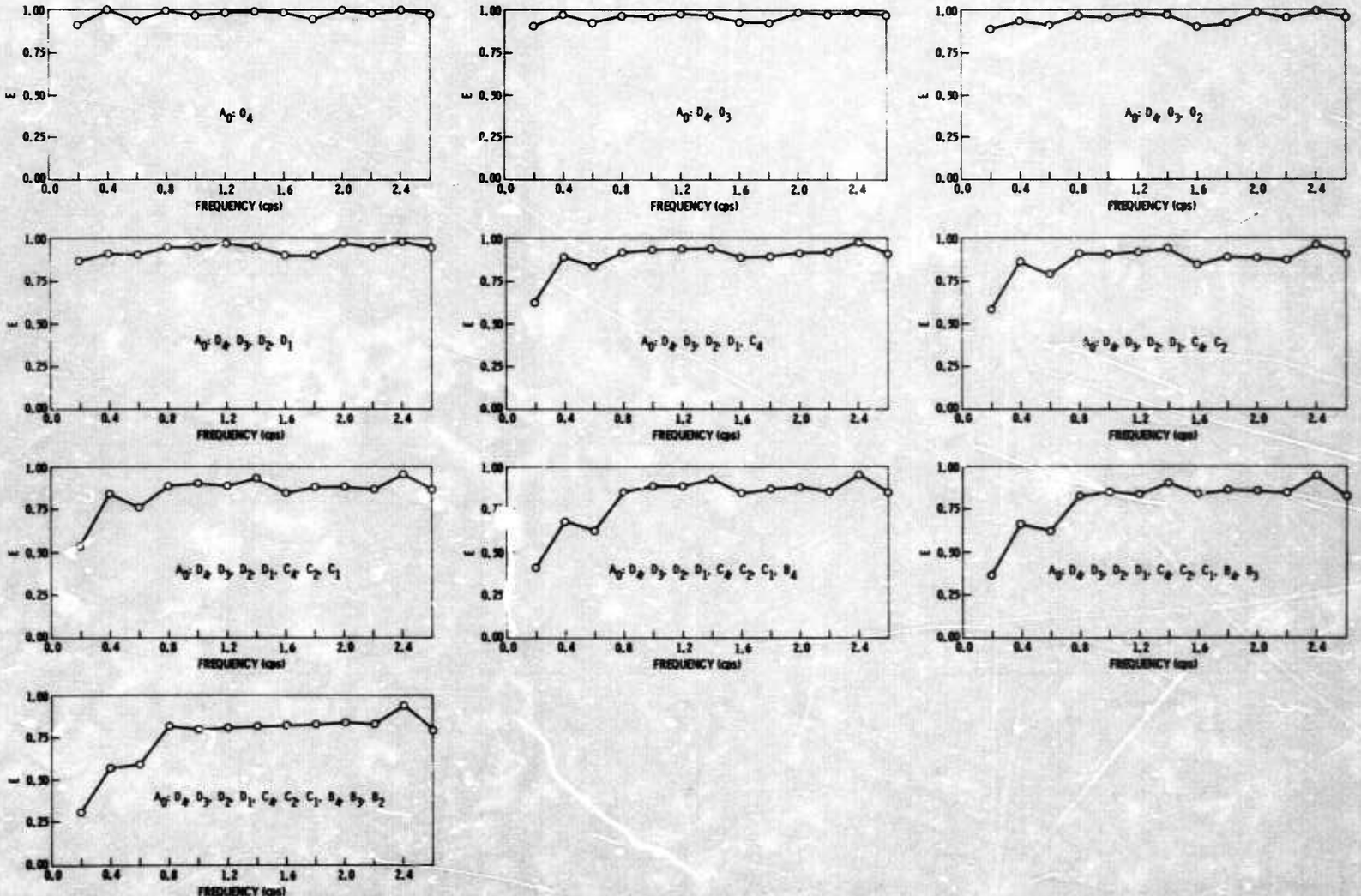

Figure V-5. Multiple Coherences, 10 November 1965

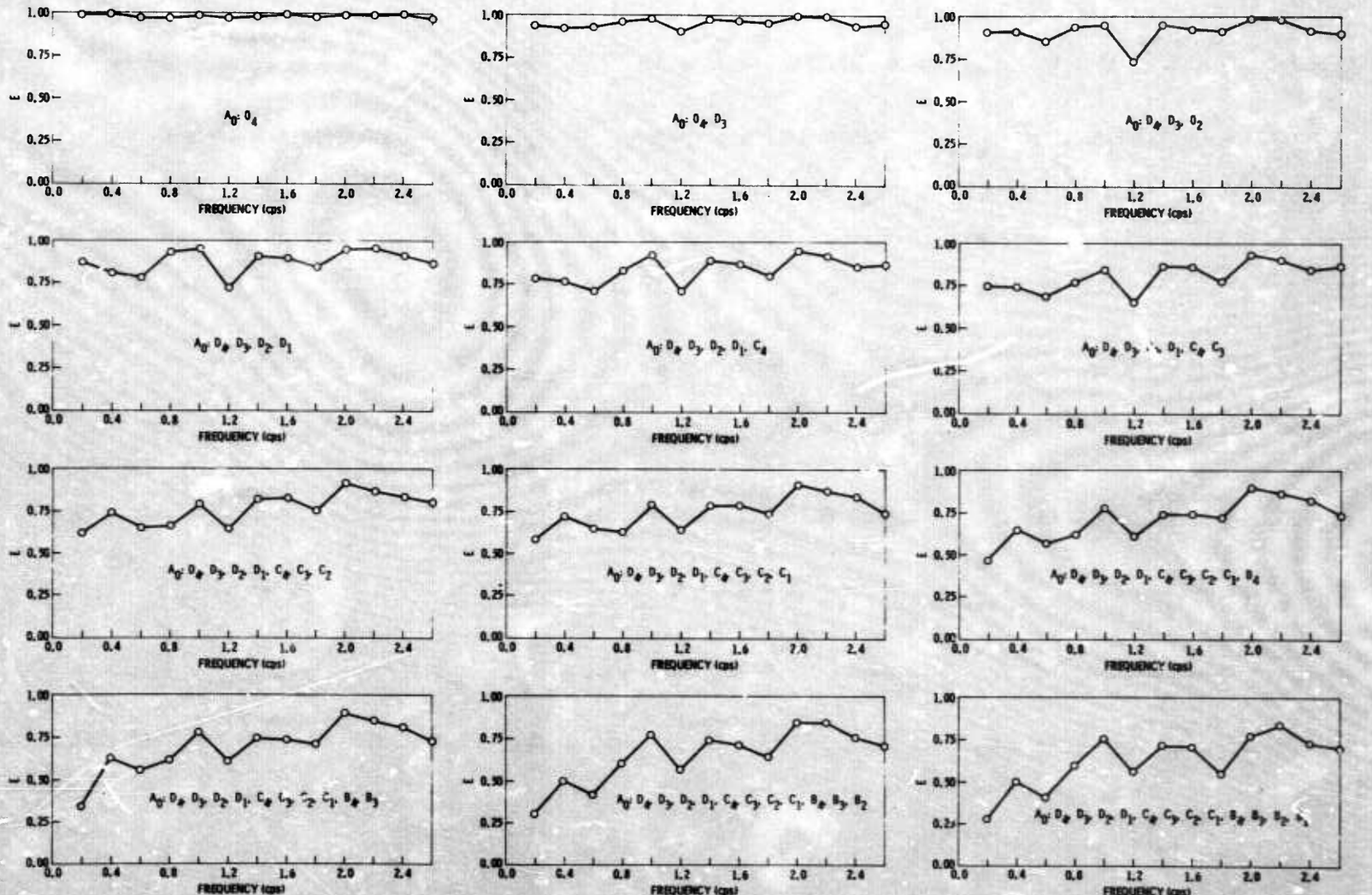

Figure V-6. Multiple Coherences, 25 November 1965

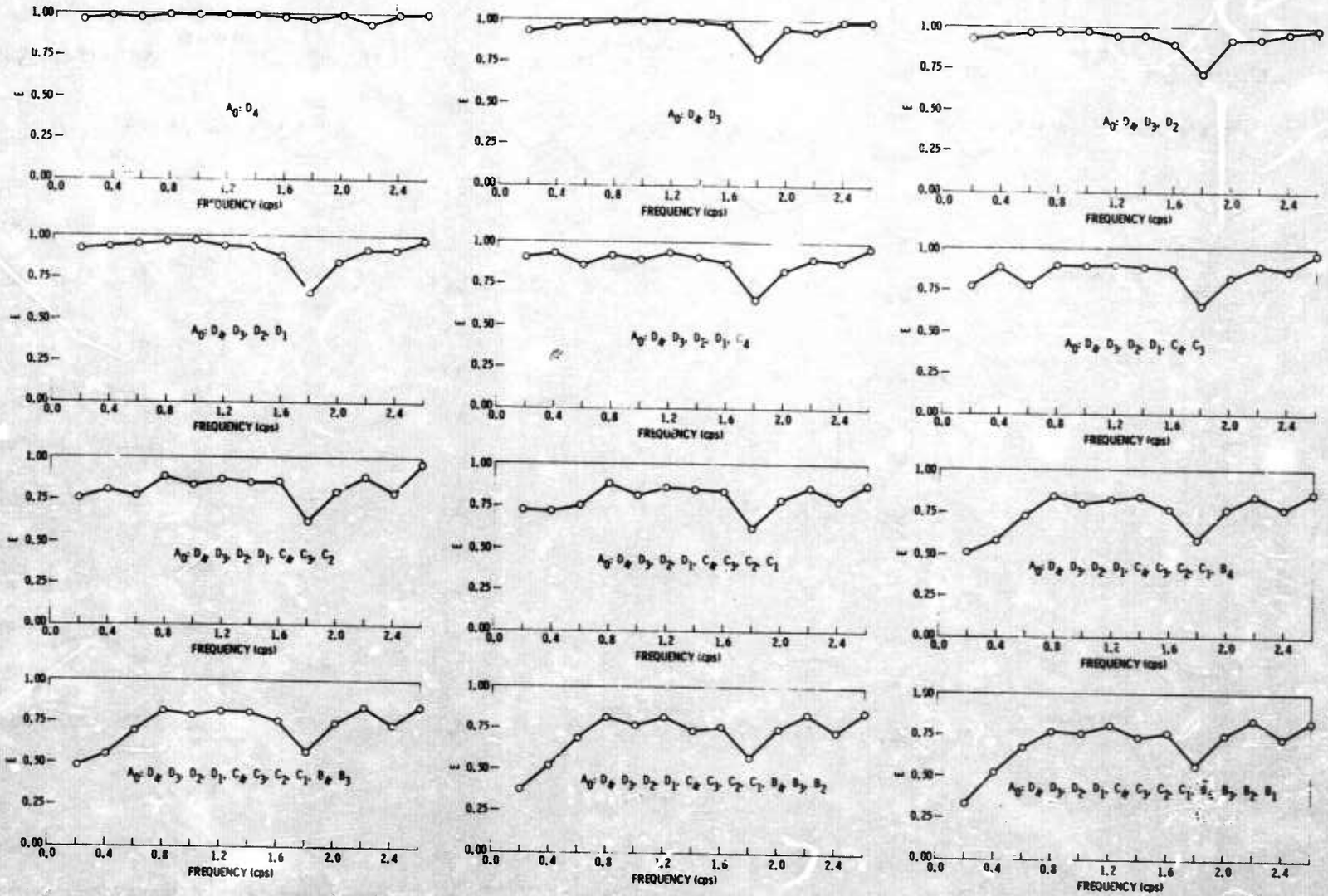

Figure V-7. Multiple Coherences, 4 December 1965

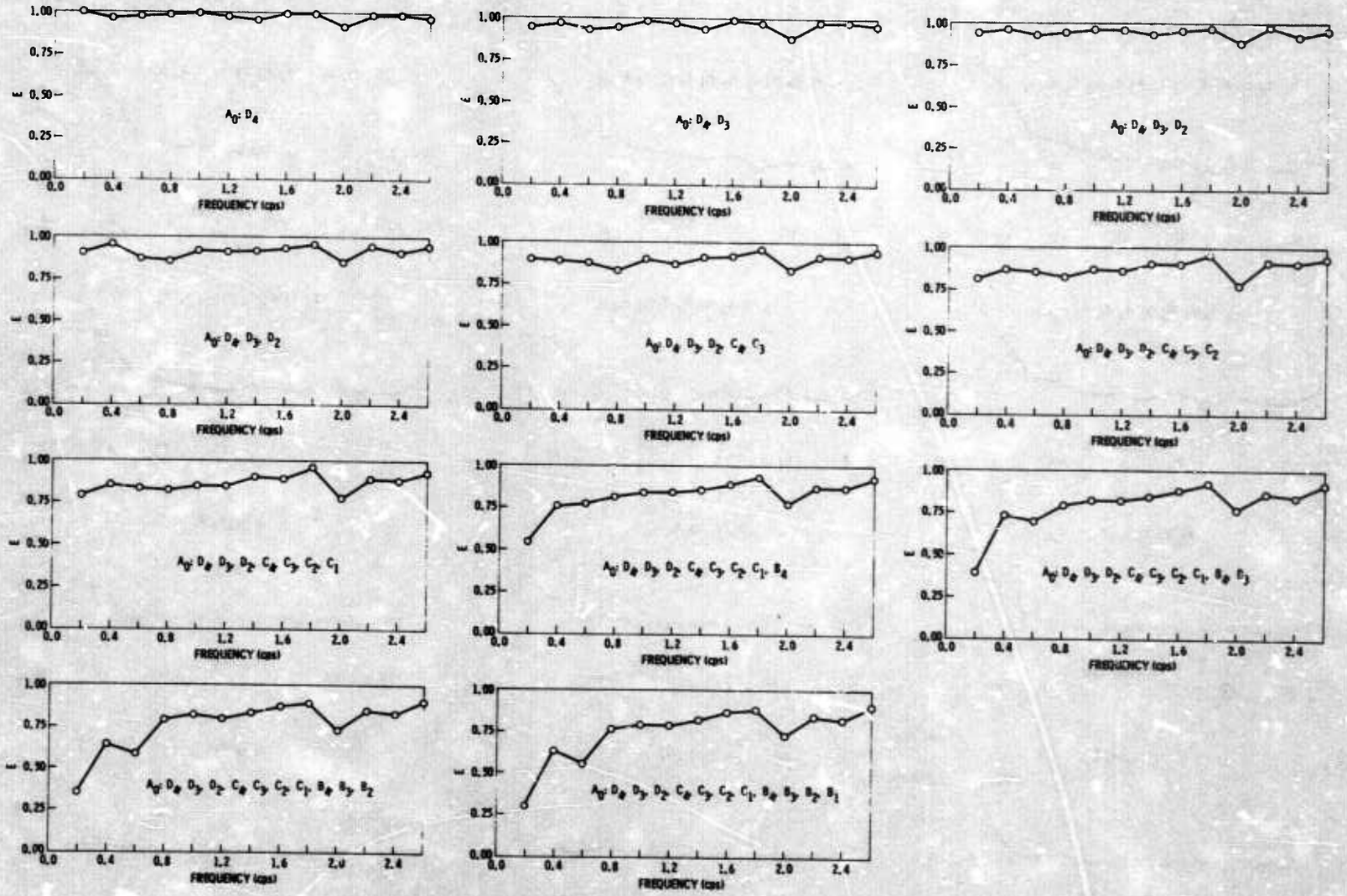

Figure V-8. Multiple Coherences, 21 December 1965

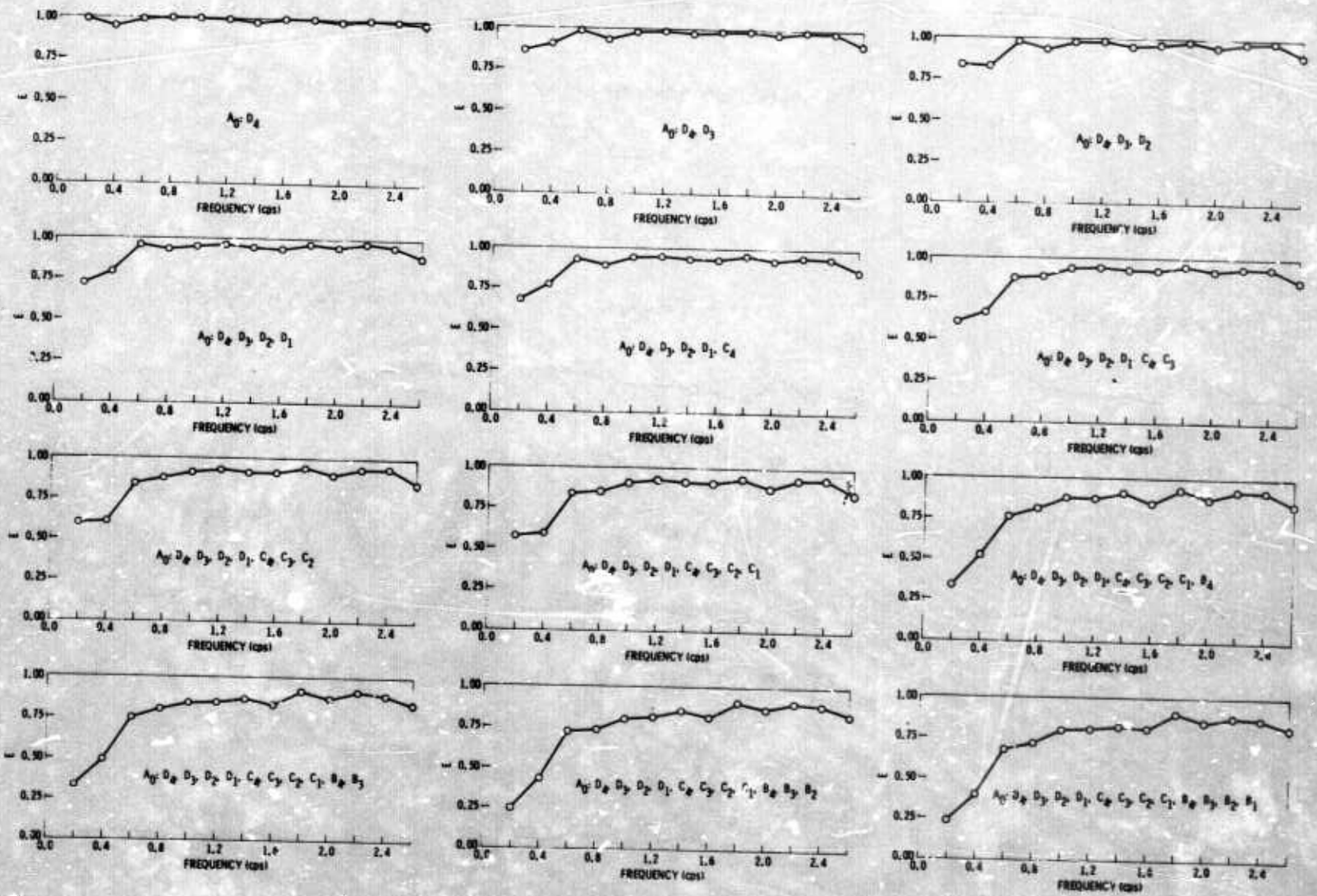

Figure V-9. Multiple Coherences, 22 January 1966

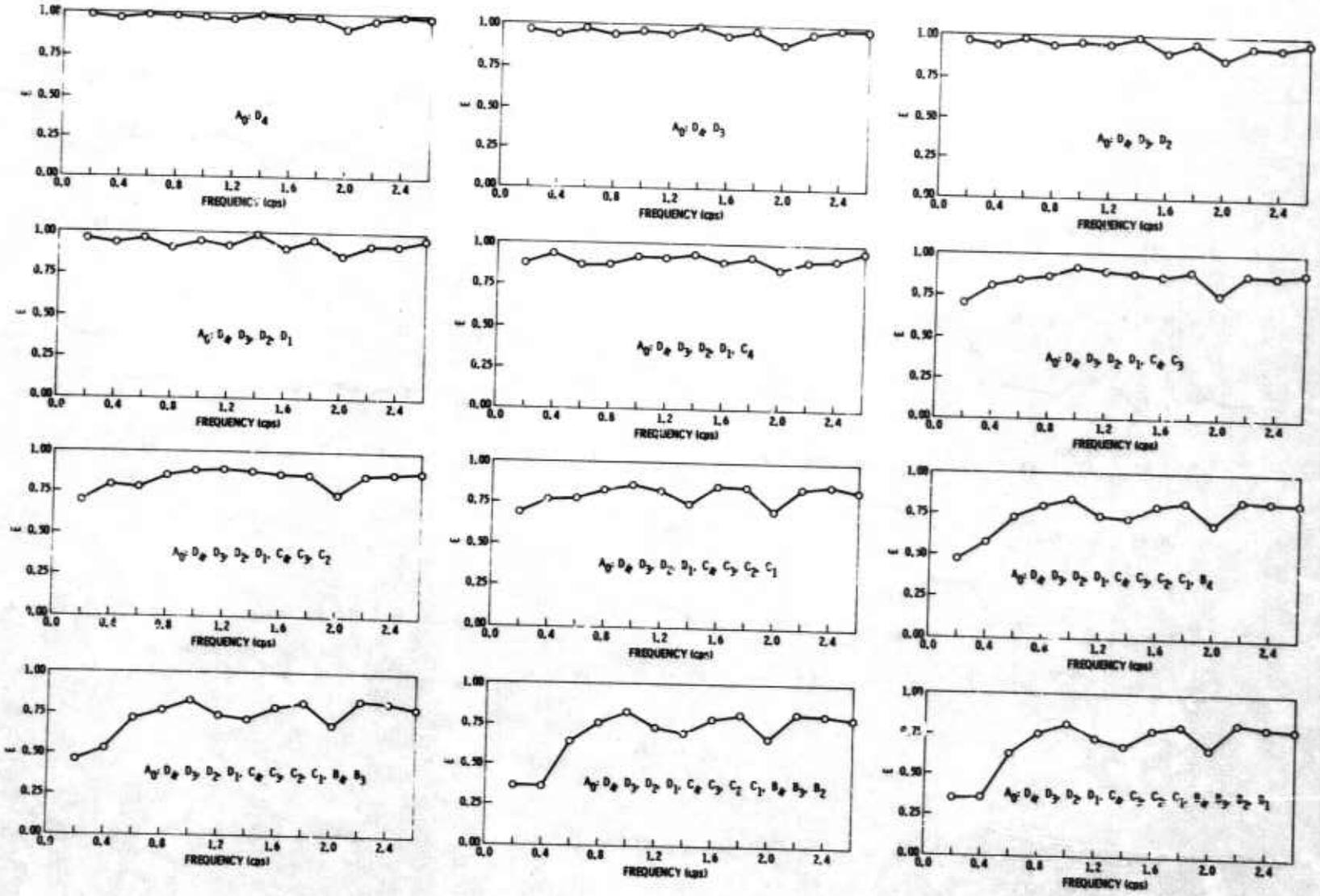

Figure V-10. Multiple Coherences, 5 February 1966

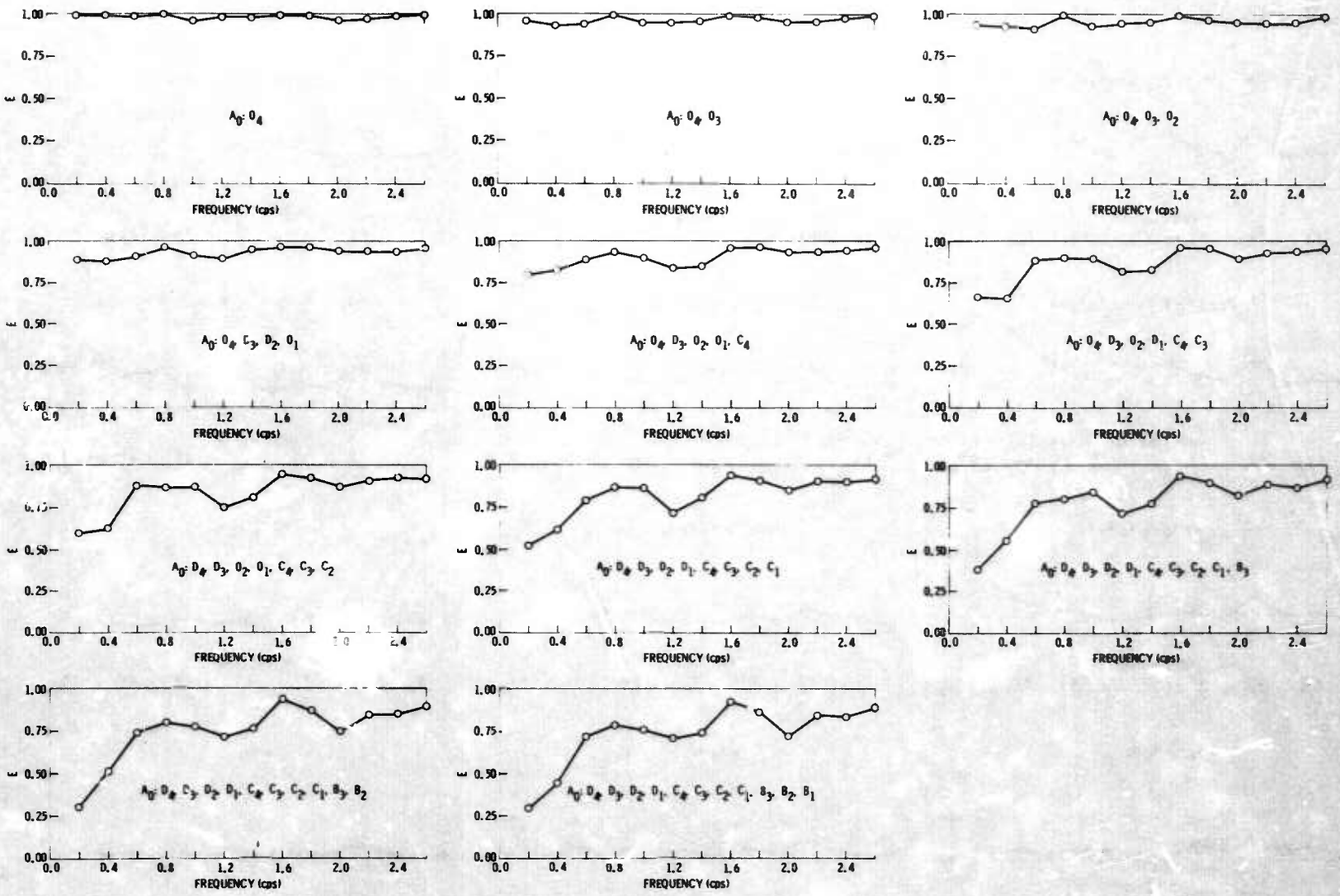

Figure V-11. Multiple Coherences, 25 March 1966

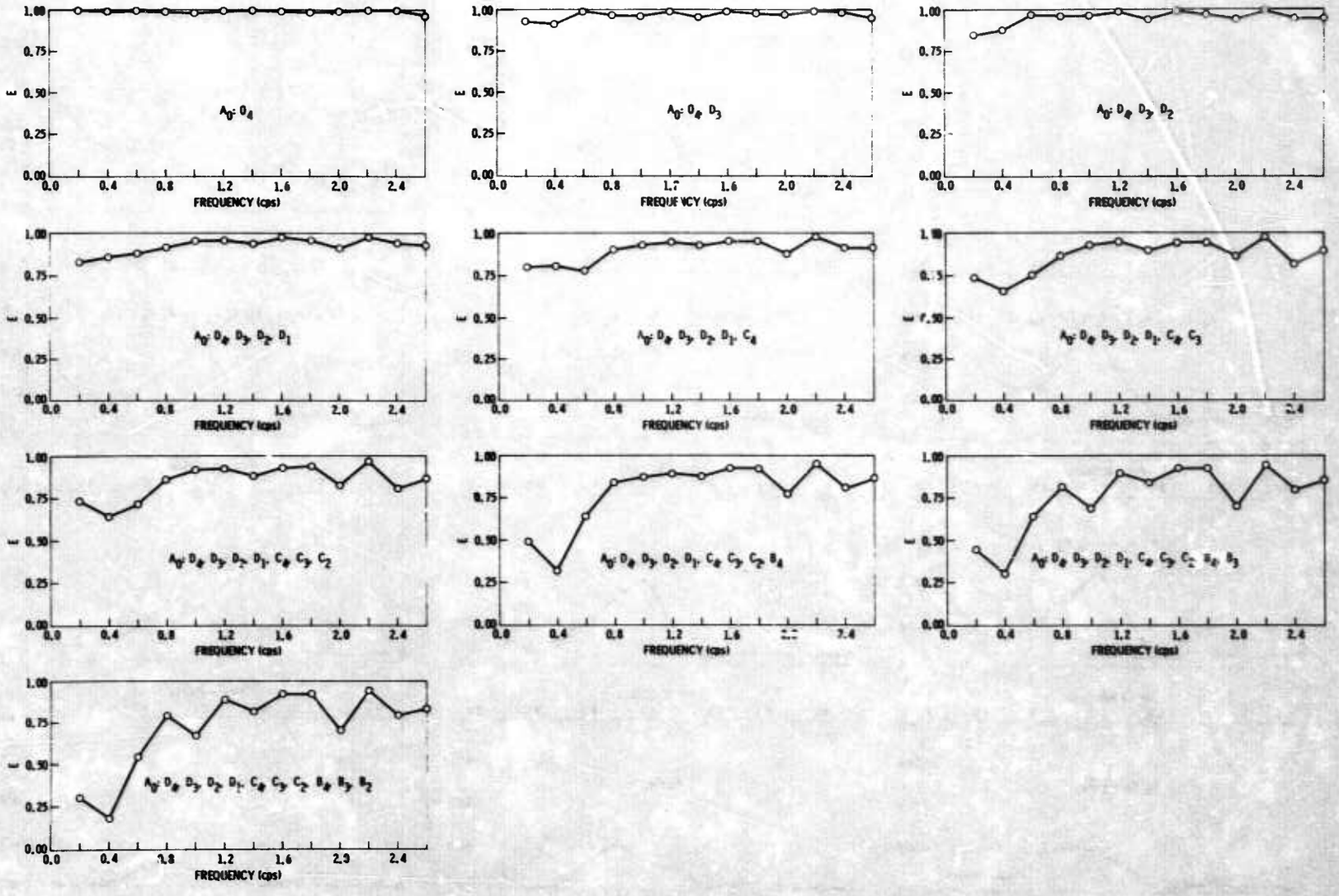

Figure V-12. Multiple Coherences, 8 April 1966

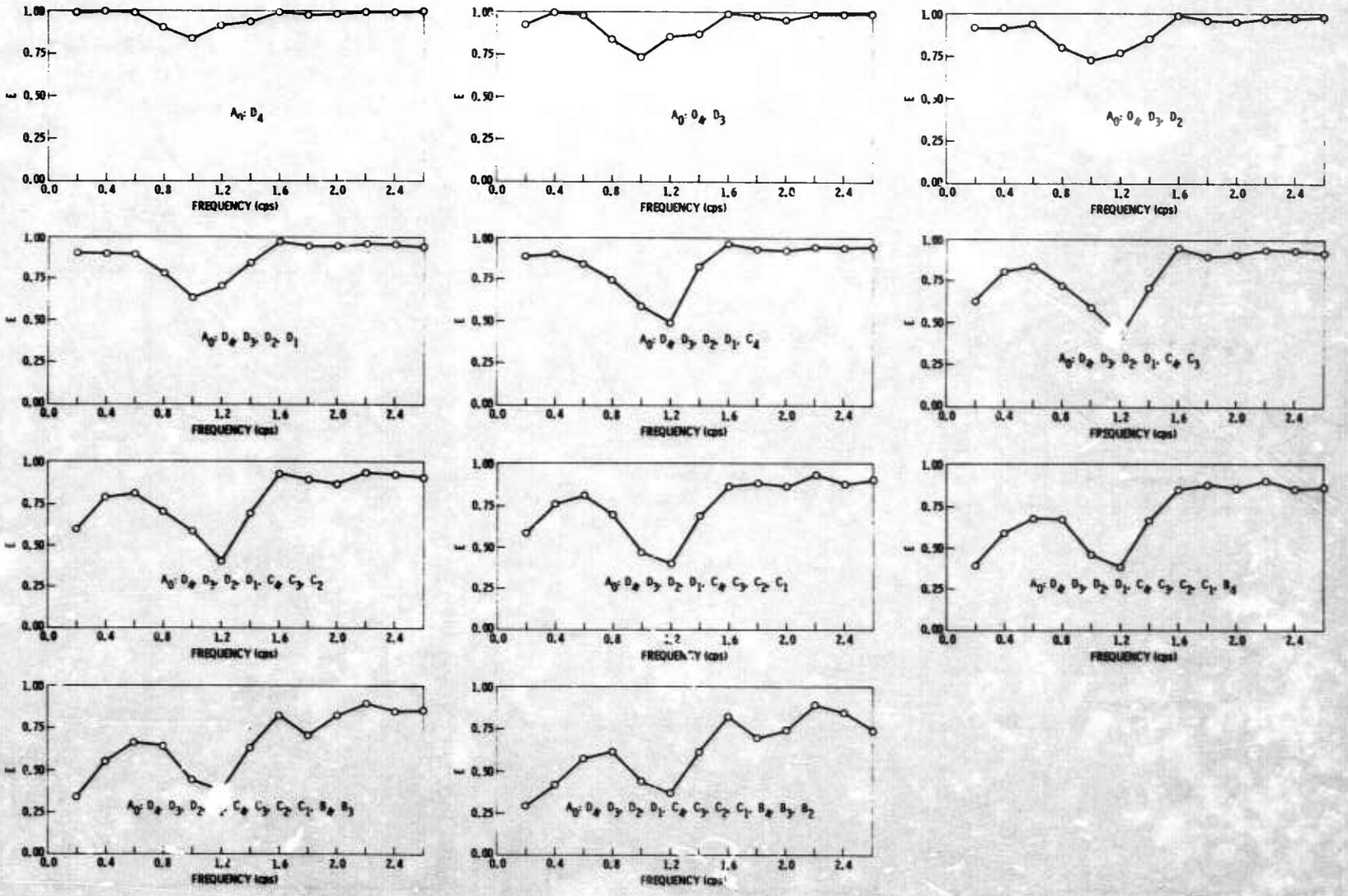

Figure V-13. Multiple Coherences, 15 April 1966

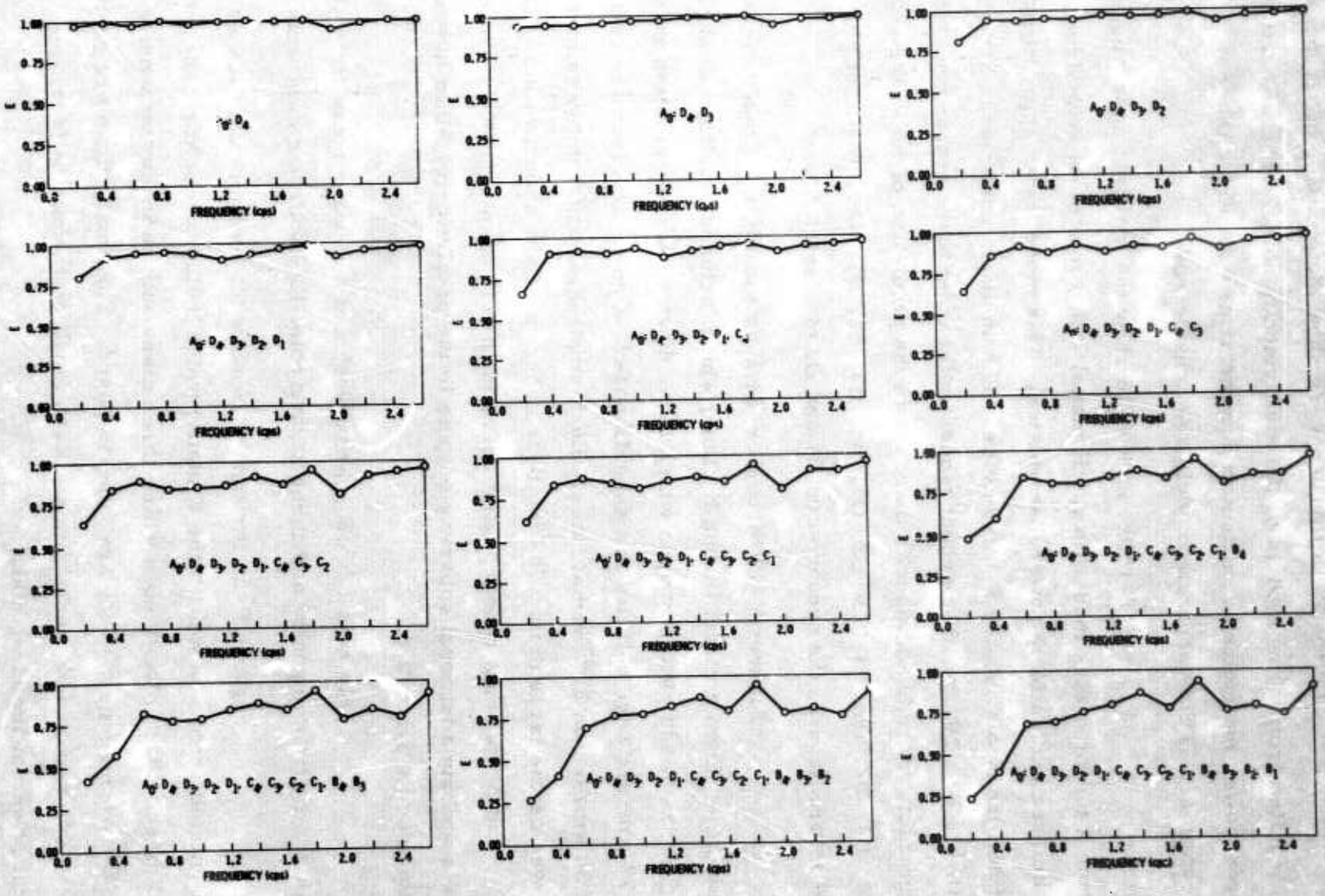

Figure V-14. Multiple Coherences, 29 April 1966

Figures V-15 through V-26 show the multiple coherences calculated from some models of the high-velocity noise. The theoretical crosspower matricies are calculated in the same manner as those in Section IV. Three separate models are considered.

Figures V-15 through V-18 show the multiple coherences from a uniform-disk model (in the K plane) with a minimum velocity of 9 km/sec and uniform power distribution. This model is an approximation of uniformly distributed P-wave noise. The multiple coherences are shown with 0-, 10-, 20-, and 50-percent random noise added to the crosspower matrix. The plots include additional subarrays in the prediction of A0 in the sequence D4, D3, D2, D1, C4, C3, C2, C1, B4, B3, B2, B1; i.e., the first plot uses D4 to predict A0, the second uses D4 and D3 to predict A0, etc.

Figures V-19 through V-22 show the multiple coherences calculated from a model (in the K plane) which includes a uniform disk with a 9-km/sec edge velocity upon which three disks with radii corresponding to a 72-km/sec edge velocity are superimposed. The small disks are centered at 36 km/sec on 120° radial lines. Each small disk contains the same total power as the large disk. The multiple coherences are shown with 0-, 10-, 20-, and 50-percent random noise added to the crosspower matrix. The plots include additional subarray outputs in the prediction of AC in the same sequence as described.

This model is an approximation of a P-wave noise field which has a uniform component and three strong point-like source components.

Figures V-23 through V-26 show the multiple coherences calculated from a model (in the K plane) which includes a uniform disk with 9-km/sec edge velocity upon which three disks with radii corresponding to a 72-km/sec edge velocity are superimposed. The small disks are centered at 36 km/sec on 120° radial lines. Each small disk contains four times the total power of the large disk.

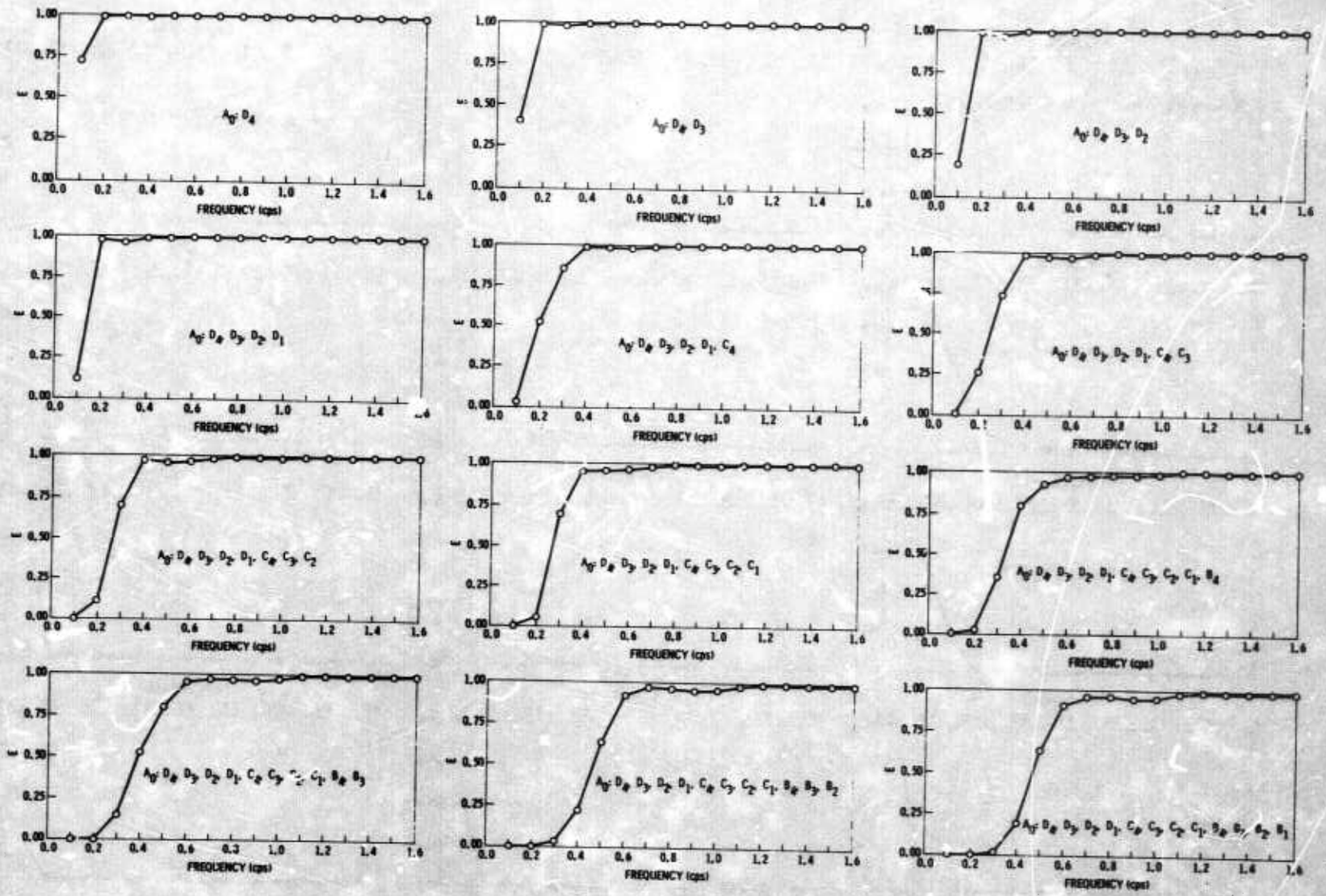

Figure V-15. Multiple Coherences for 9-km/sec Disk Model; 0-Percent Random Noise

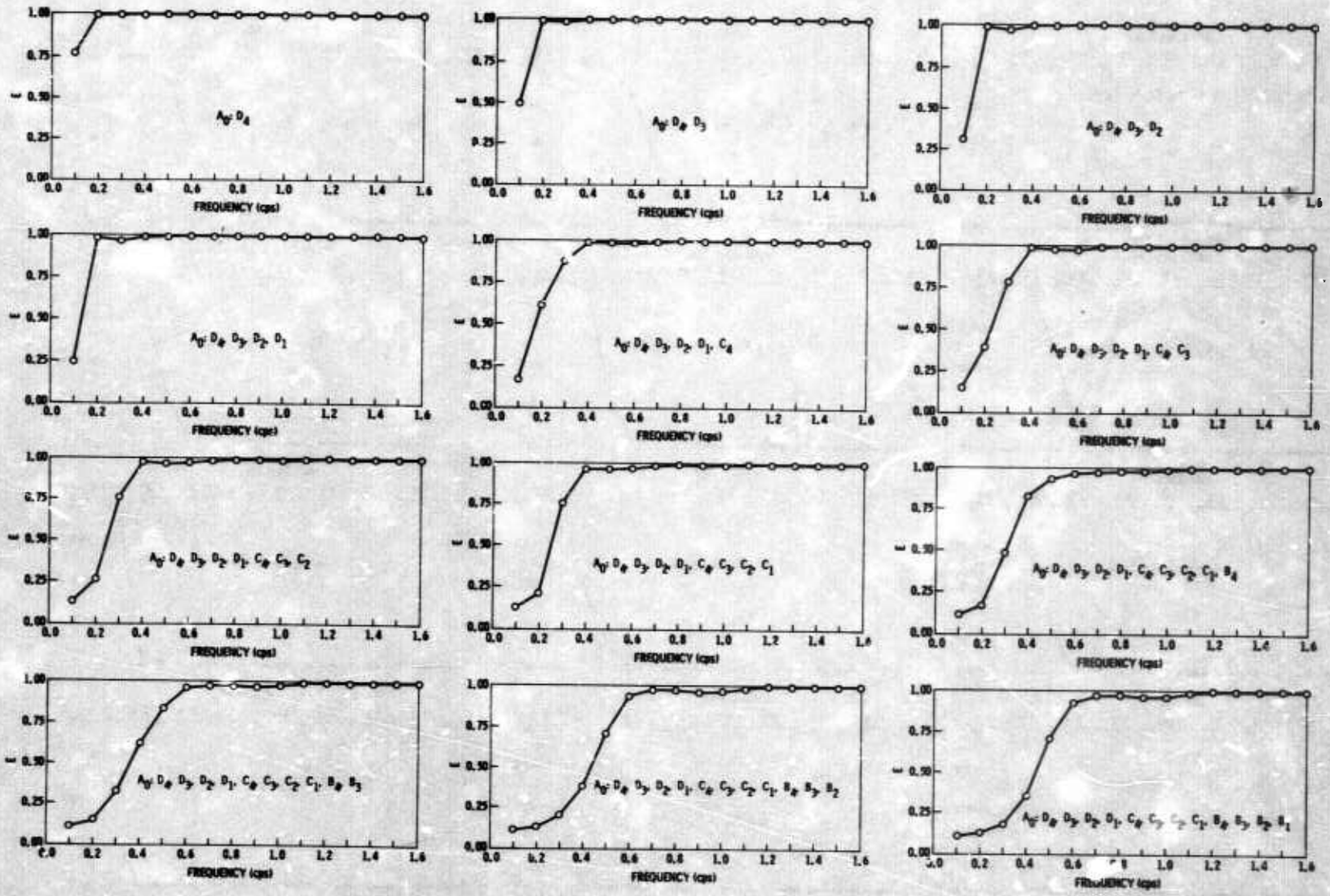

Figure V-16. Multiple Coherences for 9-km/sec Disk Model; 10-Percent Random Noise

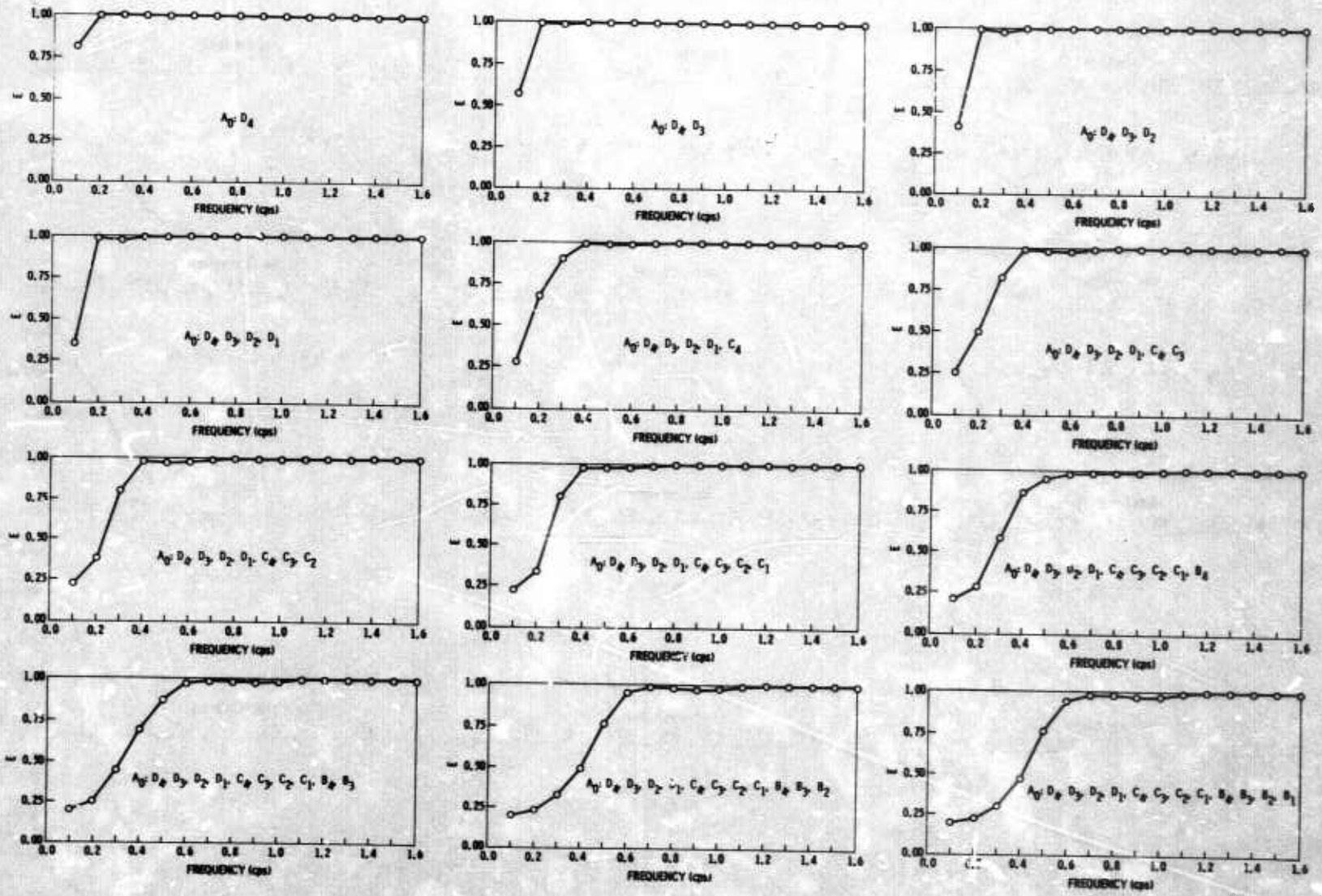

Figure V-17. Multiple Coherences for 9-km/sec Disk Model; 20-Percent Random Noise

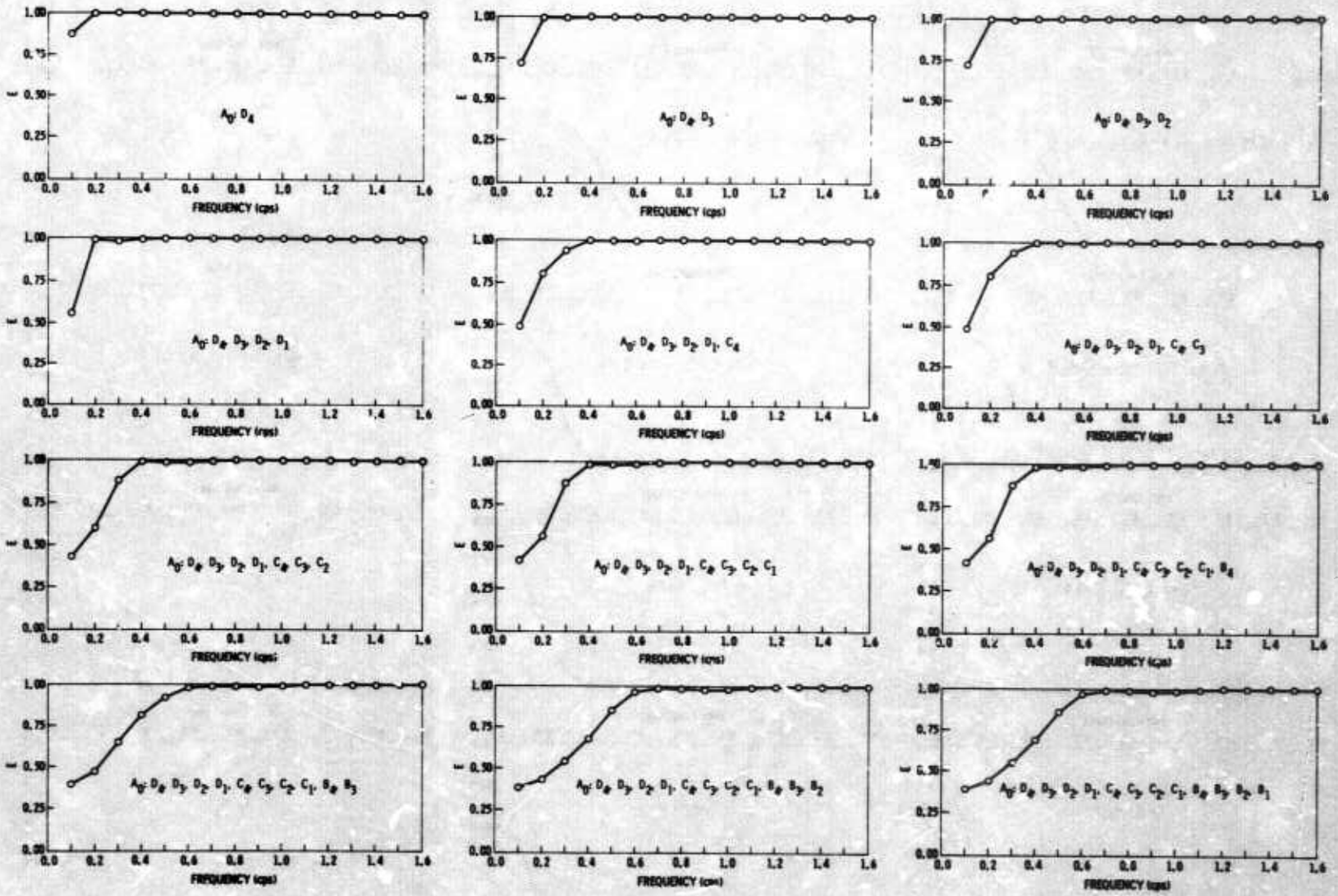

Figure V-18. Multiple Coherences for 9-km/sec Disk Model; 50-Percent Random Noise

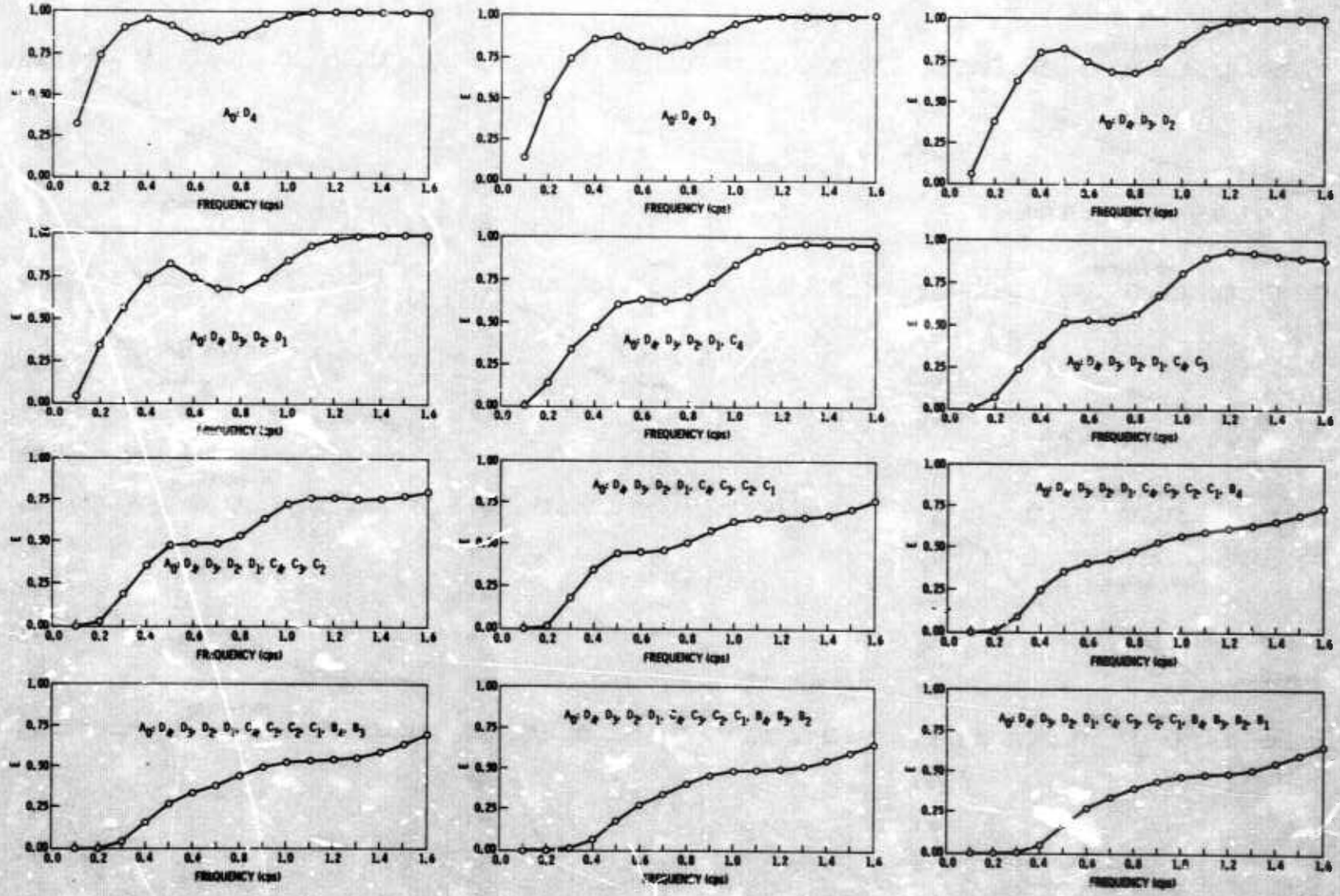

Figure V-19. Multiple Coherences for 9-km/sec Disk Model with Three 72-km/sec Disks Superimposed; 0-Percent Random Noise

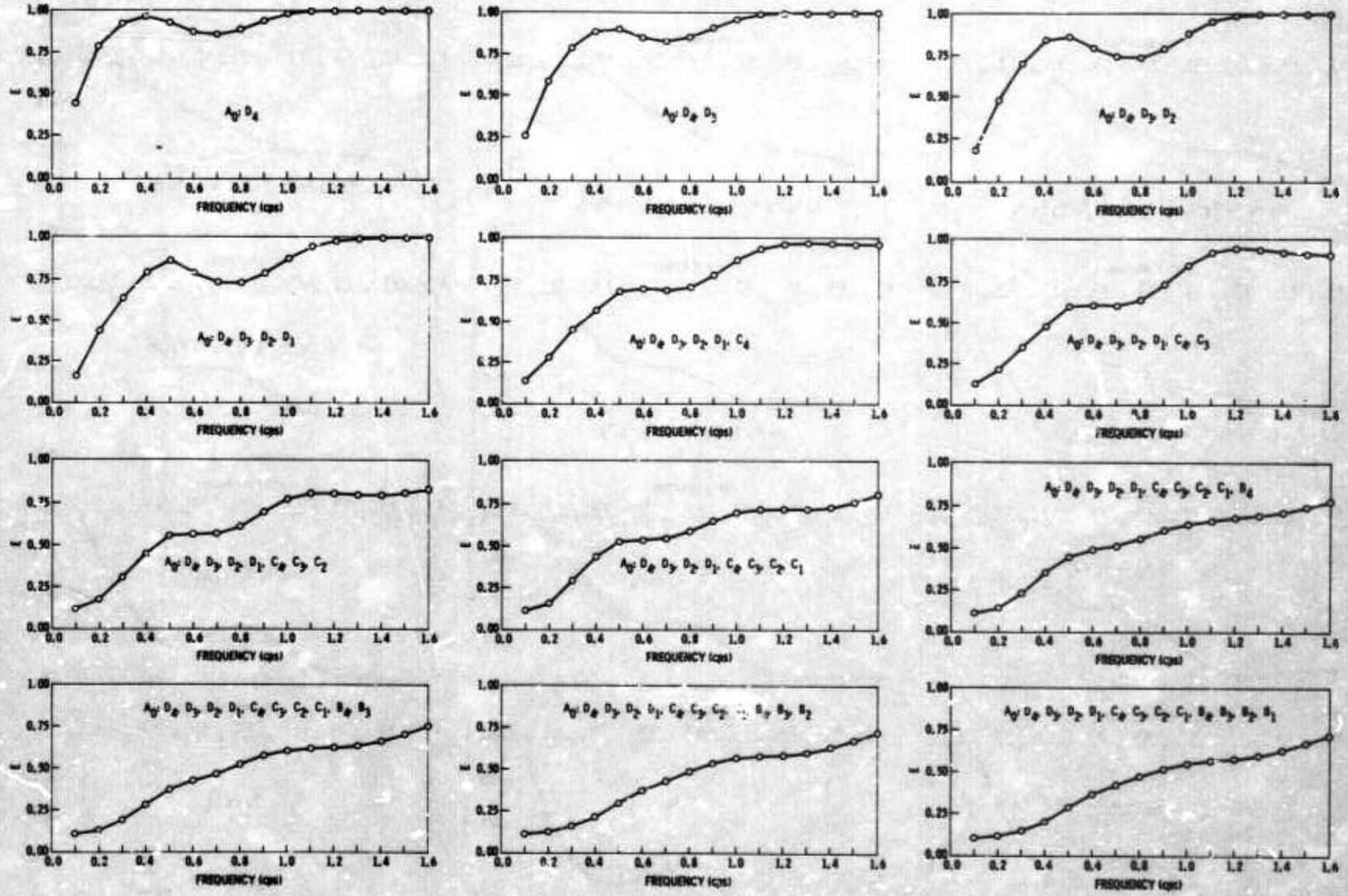

Figure V-20. Multiple Coherences for 9-km/sec Disk Model with Three 72-km/sec Disks Superimposed; 10-Percent Random Noise

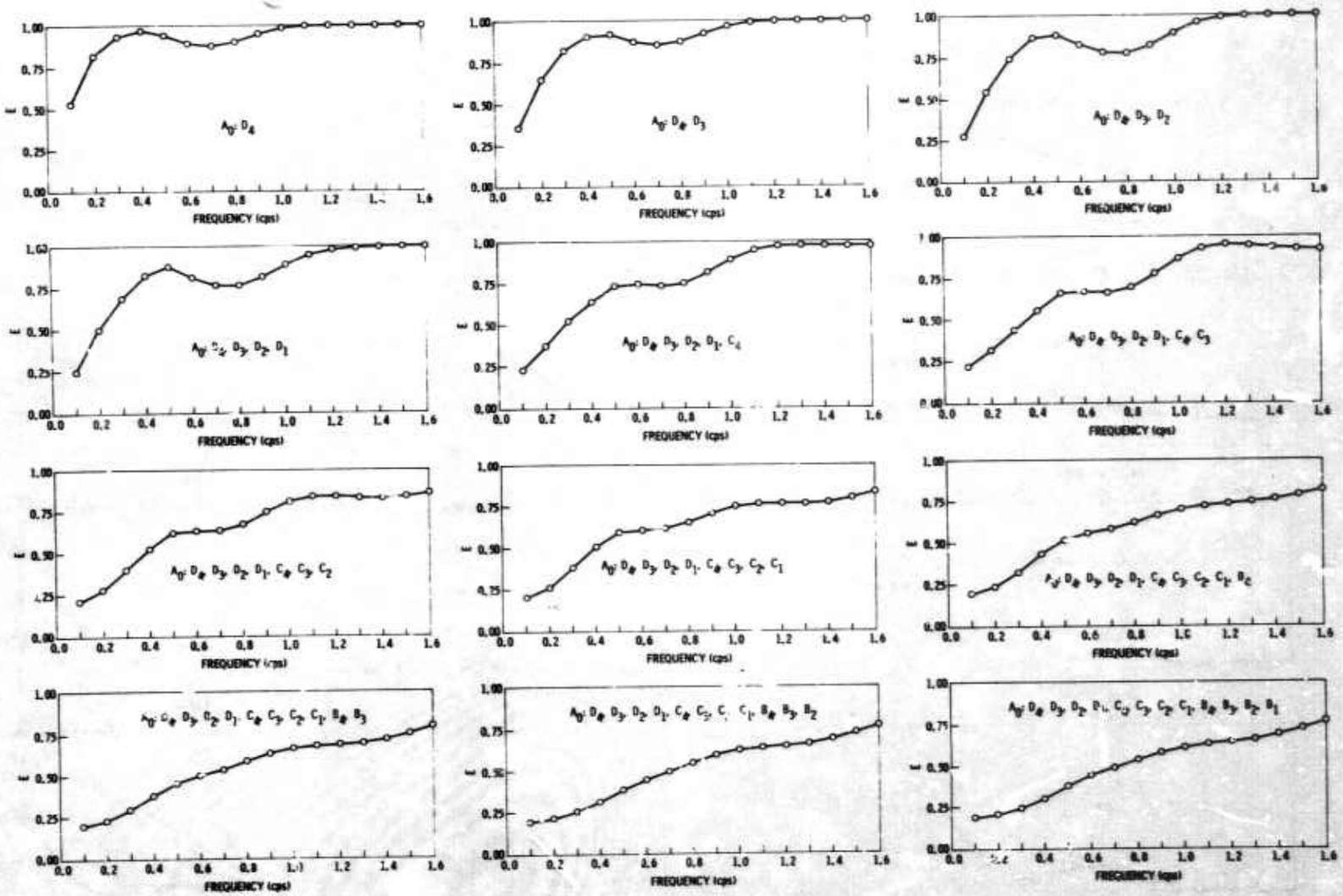

Figure V-21. Multiple Coherences for 9-km/sec Disk Model with Three 72-km/sec Disks Superimposed; 20-Percent Random Noise

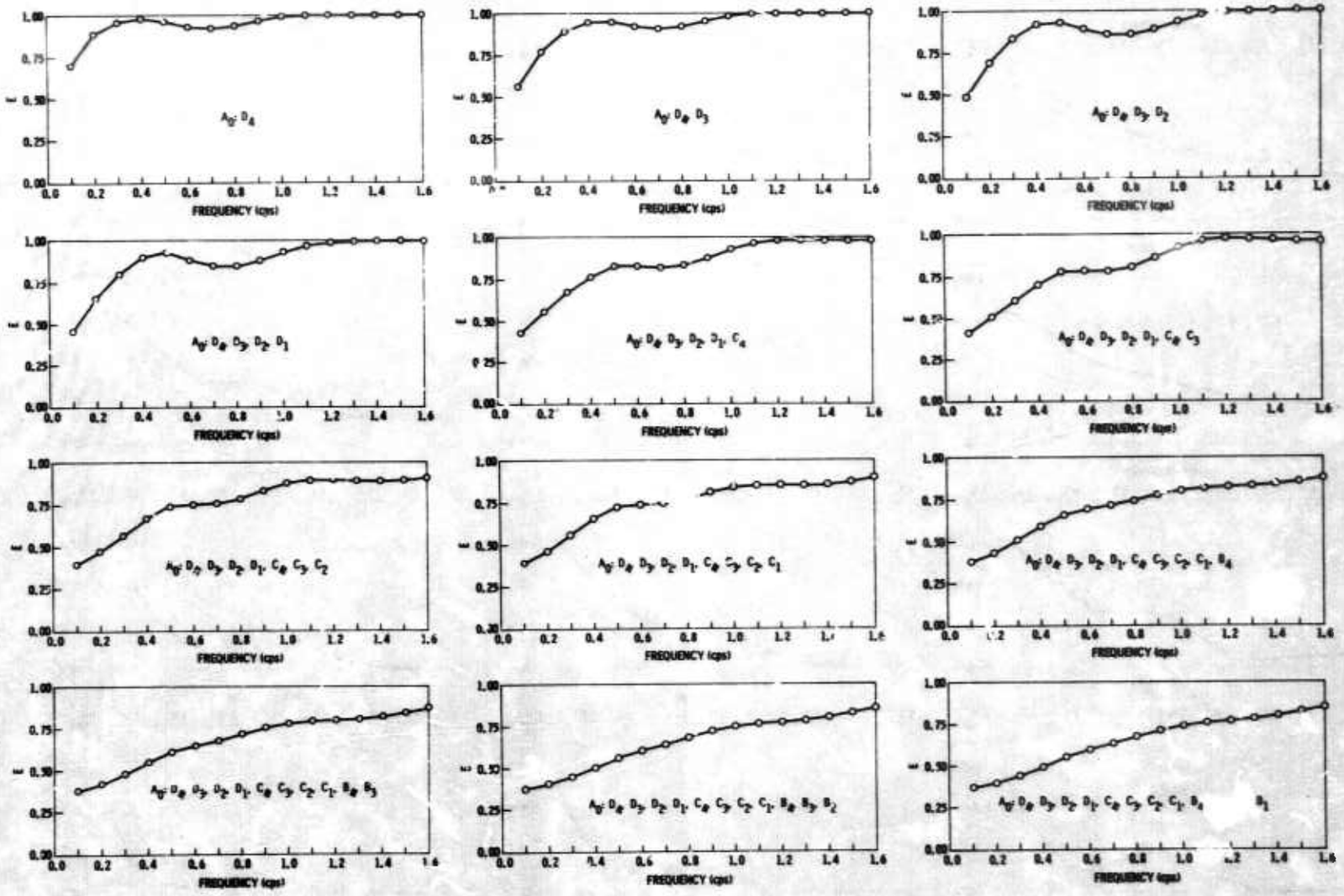

Figure V-22. Multiple Coherences for 9-km/sec Disk Model with Three 72-km/sec Disks Superimposed; 50-Percent Random Noise

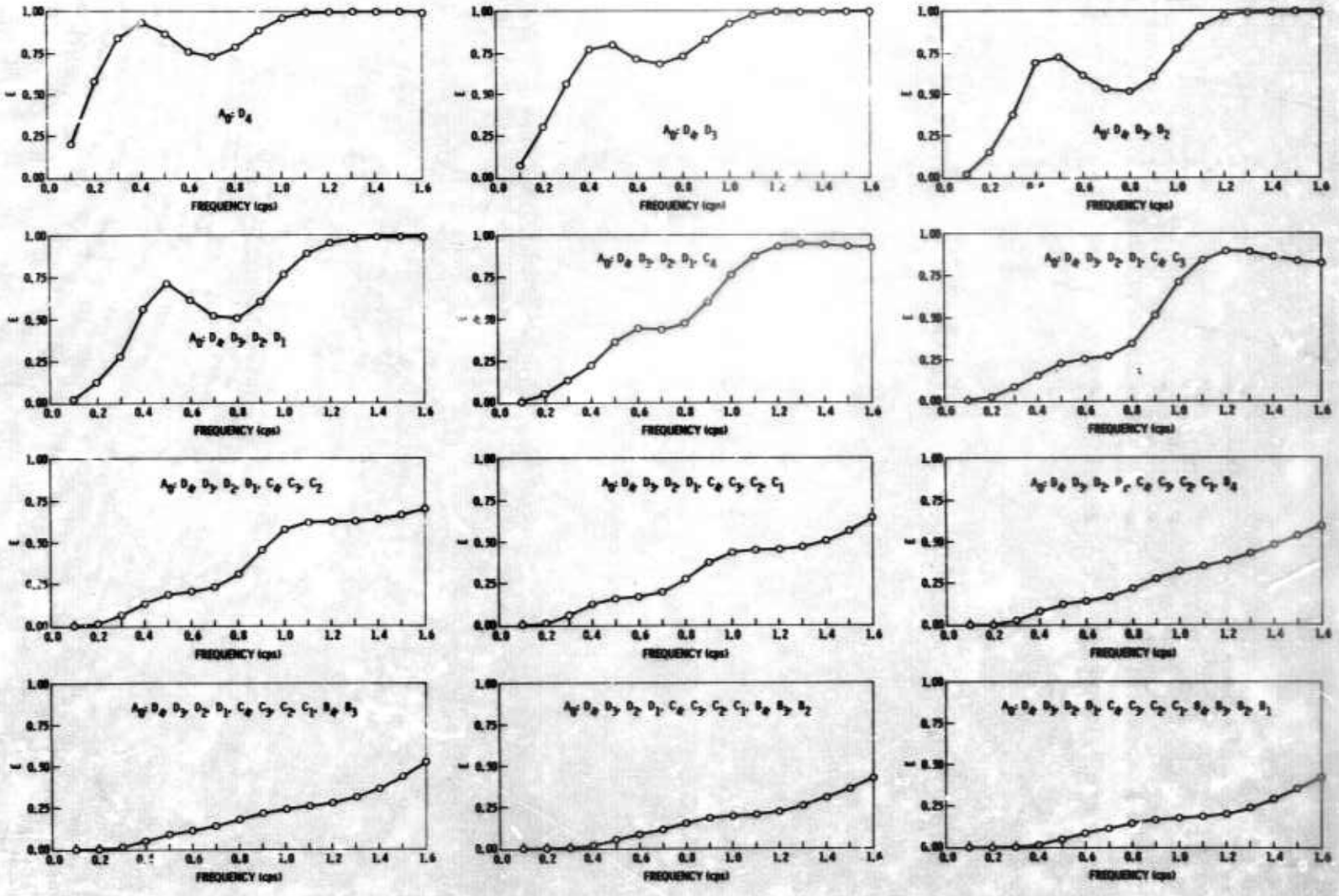

Figure V-23. Multiple Coherences for 9-km/sec Disk Model with Three 72-km/sec Disks (Scaled by 4) Superimposed; 0-Percent Random Noise

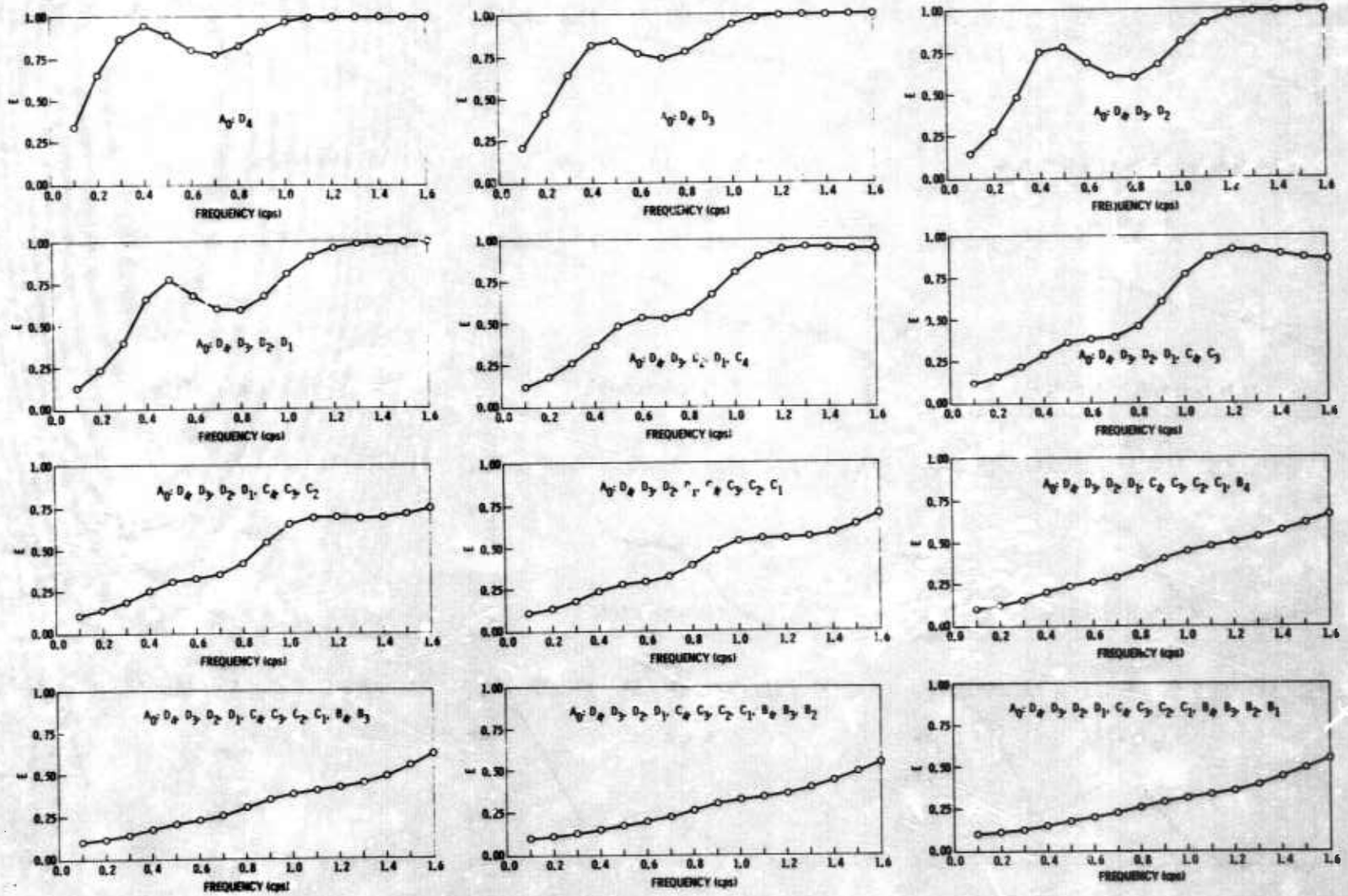

Figure V-24. Multiple Coherences for 9-km/sec Disk Model with Three 72-km/sec Disks (Scaled by 4) Superimposed; 10-Percent Random Noise

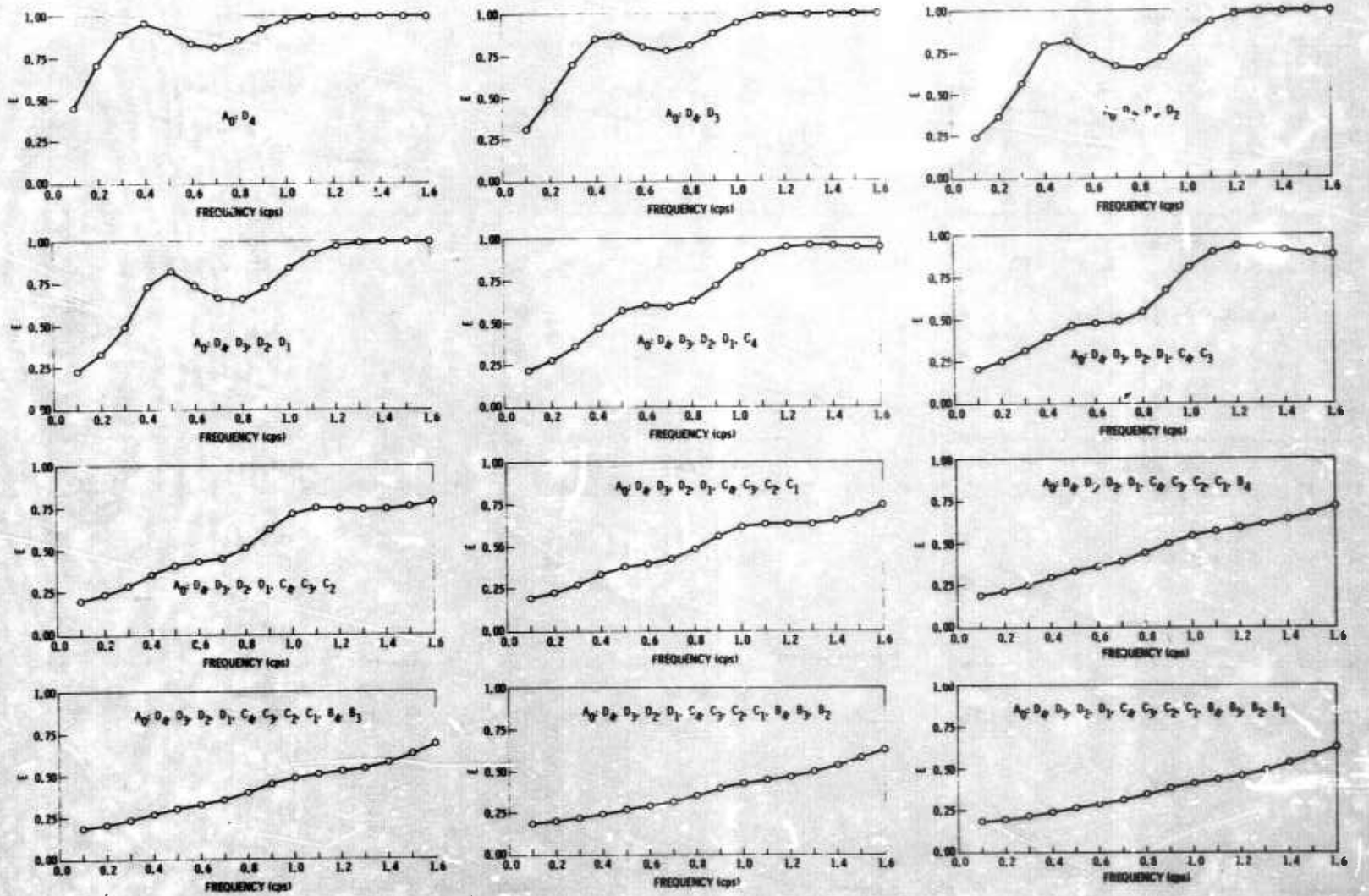

Figure V-25. Multiple Coherences for 9-km/sec Disk Model with Three 72-km/sec Disks (Scaled by 4) Superimposed; 20-Percent Random Noise

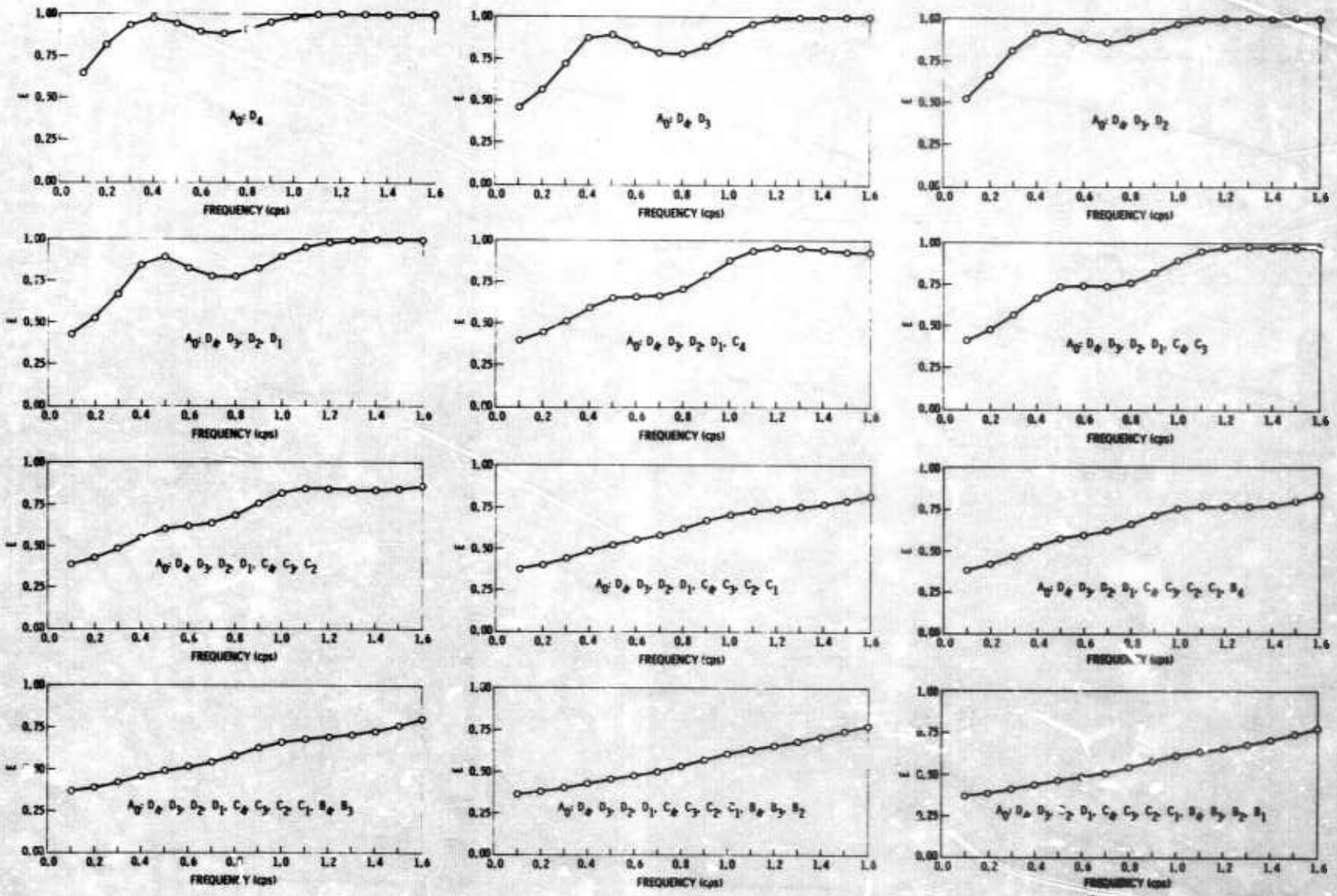

Figure V-26. Multiple Coherences for 9-km/sec Disk Model with Three 72-km/sec Disks (Scaled by 4) Superimposed; 50-Percent Random Noise

Multiple coherences are shown with 0-, 10-, 20-, and 50-percent random noise added to the crosspower matrix. The plots include additional subarray outputs in the prediction of A0 in the same sequence as described.

This model approximates a P-wave noise field which has a uniform component and three very strong point-like source components.

Study of these theoretical multiple coherences and comparison with those calculated for the LASA noise suggest the following:

- Anisotropic P-wave noise field (all lower-velocity energy having been removed by the subarray) would give strong coherence only at low frequencies ($f < 0.4$ cps) and only within the B ring of subarrays
- Three strong point-like sources superimposed on an isotropic P-wave noise field would be expected to give useful coherences only within the C ring of subarrays; it is assumed again that the subarrays eliminate the low-velocity noise and do not distort the high-velocity noise
- Three very strong point-like sources superimposed on an isotropic P-wave noise field will give good coherence between the A0 subarray and D-ring subarrays when the low-velocity noise has been effectively suppressed by the subarrays
- No broadband strong point-like sources show up in the P-wave noise as seen by using the LASA
- A strong component (at least 20 percent) of uncorrelated noise is in the subarray outputs

This incoherent component, it should be noted, may be partially due to 1.6-km/sec isotropic surface-mode noise.[5] The MCF system would pass a considerable amount of this energy.[6]

A visual fit of the models available to the LASA noise coherences shows that the one giving the best fit appears to be the 9-km/sec disk to which has been added 20- to 50-percent random noise.

SECTION VI

GROUP-COHERENCE PROGRAM

Given two sets of traces (seismometer outputs), it is desired to construct for each set a multichannel filter system which will maximize the 2-channel coherence between the two MCF outputs.

The problem can be formulated in a similar fashion for the time domain, replacing coherence by correlation. Computationally, the problem is much more tractable in the frequency domain.

Development of the group-coherence theory given here is not mathematically rigorous, since it uses the concept of the Fourier transform of a stochastic time series which is not defined. A careful mathematical development could be given, following very closely the development of the multiple coherence given by Koopmans.[1]

By taking the direct transform of N channels of time-series data, one generates (at a fixed frequency) N complex random variables having a covariance matrix Ω, which is the crosspower matrix. If the N-component complex random vector is partitioned into two sets

$$\begin{pmatrix} x^1 \\ x^2 \end{pmatrix}$$

the crosspower matrix is partioned into

$$\begin{array}{c|c} \Omega_{11} & \Omega_{12} \\ \hline \Omega_{21} & \Omega_{22} \end{array}$$

It is desired to compute linear filters which will maximize the coherence between the outputs of the two partitioned sets. If α is the vector of complex filter weights (at the fixed frequency) for the first set (X^1) and Γ is the filter-weight vector for the second set, the quantity to be maximized can be written as

$$\frac{|E(\alpha^* X^1)(\Gamma^* X^2)^*|^2}{E\left[(\alpha^* X^1)(\alpha^* X^1)^*\right] E\left[(\Gamma^* X^2)(\Gamma^* X^2)^*\right]} = \frac{|\alpha^* \Omega_{12} \Gamma|^2}{(\alpha^* \Omega_{11} \alpha)(\Gamma^* \Omega_{22} \Gamma)}$$

E denotes expected value, and * denotes conjugate transpose.

The problem also can be defined by maximizing $|\alpha^* \Omega_{12} \Gamma|$ subject to constraints $\alpha^* \Omega_{11} \alpha = 1$ and $\Gamma^* \Omega_{22} \Gamma = 1$. Since $\alpha^* \Omega_{12} \Gamma$ is complex in general, the method is to maximize the real and imaginary parts and show that they lead to the same solution.

Using the Lagrange multiplier method, we define

$$y = 1/2(\alpha^* \Omega_{12} \Gamma + \Gamma^* \Omega_{21} \alpha) - (1/2)\lambda(\alpha^* \Omega_{11} \alpha - 1) - (1/2)\mu(\Gamma^* \Omega_{22} \Gamma - 1)$$

where $(\alpha^* \Omega_{12} \Gamma + \Gamma^* \Omega_{21} \alpha)$ is twice the real part of $\alpha^* \Omega_{12} \Gamma$.

The following two lemmas are necessary to solve the problem.

Lemma 1

$$\frac{\partial}{\partial \alpha_1} \alpha^* \Omega_{11} \alpha = 2(A\alpha_1 - B\alpha_2)$$

and

$$\frac{\partial}{\partial \alpha_2} \alpha^* \Omega_{11} \alpha = 2(A\alpha_2 + B\alpha_1)$$

where

$$\Omega_{11} = A + Bi \text{ and } \alpha = \alpha_1 + \alpha_2 i$$

If we let

$$\frac{\partial}{\partial \alpha} = \frac{\partial}{\partial \alpha_1} + i \frac{\partial}{\partial \alpha_2}$$

then

$$\frac{\partial}{\partial \alpha} (\alpha^* \Omega_{11} \alpha) = 2 \Omega_{11} \alpha$$

Lemma 2

$$\frac{\partial}{\partial \alpha} (\alpha^* \Omega_{12} \Gamma + \Gamma^* \Omega_{21} \alpha) = 2 \Omega_{12} \Gamma$$

In defining

$$\frac{\partial}{\partial \alpha} = \frac{\partial}{\partial \alpha_1} + i \frac{\partial}{\partial \alpha_2}$$

note that

$$0 = \frac{\partial y}{\partial \alpha_1} = \frac{\partial y}{\partial \alpha_2} \longleftrightarrow \frac{\partial y}{\partial \alpha} = 0$$

Taking the derivatives of y with respect to α and Γ and setting them equal to 0, we arrive at

$$\Omega_{12} \Gamma - \lambda \Omega_{11} \alpha = 0 \qquad (6\text{-}1)$$

and

$$\Omega_{12}^* \alpha - \mu \Omega_{22} \Gamma = 0 \qquad (6\text{-}2)$$

Similarly, maximizing with respect to the imaginary part of the coherence, we define

$$y' = \frac{1}{2i} (\alpha^* \Omega_{12} \Gamma - \Gamma^* \Omega_{21} \alpha) - \frac{1}{2} \lambda' (\alpha^* \Omega_{11} \alpha - 1) - \frac{1}{2} \mu' (\Gamma^* \Omega_{22} \Gamma - 1)$$

Using the lemma

$$\frac{\partial}{\partial \alpha} \left[\left(\frac{1}{2i} \right) (\alpha^* \Omega_{12} \Gamma - \Gamma^* \Omega_{21} \alpha) \right] = -i \Omega_{12} \Gamma$$

and setting the derivatives of y' with respect to α and Γ equal to 0, we derive

$$-i \Omega_{12} \Gamma - \lambda' \Omega_{11} \alpha = 0 \qquad (6\text{-}3)$$

and

$$i \Omega_{12} \alpha - \mu' \Omega_{22} \Gamma = 0 \qquad (6\text{-}4)$$

Multiplying Equation (6-1) by α^* and Equation (6-2) by Γ^* and applying the constraints $\alpha^* \Omega_{11} \alpha = 1$ and $\Gamma^* \Omega_{22} \Gamma = 1$, we derive

$$\alpha^* \Omega_{12} \Gamma = \lambda$$

and

$$\Gamma^* \Omega_{21} \alpha = \mu$$

In other words, $\lambda = \mu^*$ and the coherence

$$\frac{|\alpha^* \Omega_{12} \Gamma|^2}{(\alpha^* \Omega_{11} \alpha)(\Gamma^* \Omega_{22} \Gamma)} = |\lambda| = |\mu|^2$$

Multiplying Equation (6-2) by Ω_{22}^{-1}, we get

$$\Omega_{22}^{-1} \Omega_{21} \alpha = \lambda^* \Gamma$$

or

$$\Gamma = \frac{\Omega_{22}^{-1} \Omega_{21} \alpha}{\lambda^*} \tag{6-5}$$

Multiplying Equation (6-1) by λ^*, we have

$$\lambda^* \Omega_{12} \Gamma = \lambda \lambda^* \Omega_{11} \alpha \tag{6-6}$$

Using Equation (6-5) in Equation (6-6), we derive

$$\Omega_{12} \Omega_{22}^{-1} \Omega_{21} \alpha = \lambda \lambda^* \Omega_{11} \alpha$$

which is a generalized eigenvalue problem that can be solved for the coherence ($|\lambda|^2$) and the filtering weights (α), which are the components of the associated eigenvector.

Operating similarly on Equations (6-3) and (6-4), we arrive at

$$-i\alpha^* \Omega_{12} \Gamma = \lambda'$$

and

$$i\Gamma^* \Omega_{21} \alpha = \mu'$$

or

$$\lambda' = \mu'^*$$

and

$$|\lambda'|^2 = |\mu'|^2$$

Multiplying Equation (6-4) from the left by Ω_{22}^{-1}, we have

$$\frac{i\,\Omega_{22}^{-1}\,\Omega_{21}\alpha}{\lambda'^{*}} = \Gamma \qquad (6\text{-}7)$$

and multiplying Equation (6-3) by λ'^{*} gives

$$-i\,\lambda'^{*}\,\Omega_{12}\,\Gamma = \lambda'^{*}\,\lambda'\,\Omega_{11}\alpha \qquad (6\text{-}8)$$

Using Equation (6-7) in Equation (6-8), we derive

$$\Omega_{12}\,\Omega_{22}^{-1}\,\Omega_{21}\,\alpha = |\lambda'|^{2}\,\Omega_{11}\,\alpha \qquad (6\text{-}9)$$

which is the same problem arrived at when setting the derivatives of $y = 0$. Thus, maximizing with respect to the real or imaginary part of the coherence is equivalent to maximizing with respect to the absolute value.

The eigenvalue problem to be solved is thus reduced to

$$(\Omega_{12}\,\Omega_{22}^{-1}\,\Omega_{21} - |\lambda|^{2}\,\Omega_{11})\alpha = 0 \qquad (6\text{-}10)$$

or

$$(\Omega_{11}^{-1}\,\Omega_{12}\,\Omega_{22}^{-1}\,\Omega_{21} - |\lambda|^{2}\,I)\,\alpha = 0 \qquad (6\text{-}11)$$

Note that, since the partition of a covariance matrix is

$$\left[\begin{array}{c|c} \Omega_{11} & \Omega_{12} \\ \hline \Omega_{21} & \Omega_{22} \end{array}\right]$$

Ω_{11}, Ω_{11}^{-1}, Ω_{22}, and Ω_{22}^{-1} are positive definite; also since $\Omega_{12} = \Omega_{21}^{*}$, $(\Omega_{12}\Omega_{22}^{-1}\Omega_{21})$ is positive definite. Since $(\Omega_{12}\Omega_{22}^{-1}\Omega_{21})$ and Ω_{11} are positive definite, there exists a nonsingular matrix F such that

$$F^{*}(\Omega_{12}\,\Omega_{22}^{-1}\,\Omega_{21})\,F = \begin{bmatrix} |\lambda_1|^2 & \cdots & 0 \\ \vdots & \ddots & \\ 0 & & |\lambda_p| \end{bmatrix} = \mathbf{\Lambda}$$

where $\mathbf{\Lambda}$ is the matrix of eigenvalues of Equation (6-10) arranged so that $|\lambda_i| \leq |\lambda_j|$ for $j < i$ and

$$F^{*}\,\Omega_{11}\,F = I$$

where I is the identity matrix.

Since $F^{*}\,\Omega_{12}\,\Omega_{22}^{-1}\,\Omega_{21}\,F = \mathbf{\Lambda}$ and $F^{*}\,\Omega_{11}\,F = I$, we have

$$F^{*}\,\Omega_{12}\,\Omega_{22}^{-1}\,\Omega_{21}\,F = F^{*}\,\Omega_{11}\,F\,\mathbf{\Lambda}$$

and thus

$$\Omega_{12}\,\Omega_{22}^{-1}\,\Omega_{21}\,F = \Omega_{11}\,F\,\mathbf{\Lambda} \qquad (6\text{-}12)$$

Since $\mathbf{\Lambda}$ is a diagonal matrix,

$$\Omega_{12}\,\Omega_{22}^{-1}\,\Omega_{21}\,f_i = \Omega_{11}\,f_i\,|\lambda_i|^2$$

where f_i is the i^{th} column of F and $|\lambda_i|^2$ is the i^{th} eigenvalue.

Thus, F is the matrix with columns that are the eigenvectors of Equation (6-10). Note that, from Equation (6-12), we have

$$\Omega_{11}^{-1}\,\Omega_{12}\,\Omega_{22}^{-1}\,\Omega_{21} = F\,\Lambda\,F^{-1} \qquad (6\text{-}13)$$

which will be useful in the following equations.

The problem [Equation (6-10)] is solved by an iteration commonly known as the power method. Taking a starting solution vector of

$$\alpha(0) = \left(\frac{1}{n}, \ldots, \frac{1}{n}\right)^T$$

and defining

$$\alpha(N+1) = \frac{\Omega_{11}^{-1}\,\Omega_{12}\,\Omega_{22}^{-1}\,\Omega_{21}\,\alpha(N)}{\left[\alpha^*(N)\,\alpha(N)\right]^{1/2}} = \Omega_{11}^{-1}\,\Omega_{12}\,\Omega_{22}^{-1}\,\Omega_{21}\,\beta(N)$$

where

$$\beta(N) = \frac{\alpha(N)}{|\alpha(N)|} \qquad (6\text{-}14)$$

the result of N iterations is

$$\beta(N) = C_N(\Omega_{11}^{-1}\,\Omega_{12}\,\Omega_{22}^{-1}\,\Omega_{21})^N\,\alpha(0)$$

where

$$C_N = \frac{1}{\prod_{i=0}^{N-1} |\alpha_i|} = C_N(F\,\Lambda\,F^{-1})^N\,\alpha(0) \qquad \text{[from Equation (6-13)]}$$

$$= C_N F(\Lambda)^N F^{-1}\,\alpha(0) = C_N\,|\lambda_1|^{2N}\,F\,\frac{1}{|\lambda_1|^{2N}}\,(\Lambda)^N F^{-1}\,\alpha(0)$$

If $\lambda_1 > \lambda_2 \geq \lambda_3 \ldots . \geq \lambda_\rho$, then

$$\frac{1}{|\lambda_1|^{2N}} (\Lambda)^N = \begin{bmatrix} 1 & 0 & \cdot & \cdot & \cdot & 0 \\ 0 & \left|\frac{\lambda_2}{\lambda_1}\right|^{2N} & & & & \\ \cdot & & \cdot & & & \\ \cdot & & & \cdot & & \\ \cdot & & & & \cdot & \\ \cdot & & & & & \\ 0 & & & & & \left|\frac{\lambda_\rho}{\lambda_1}\right|^{2N} \end{bmatrix}$$

As $N \to \infty$, this approaches the matrix

$$\begin{bmatrix} 1 & 0 & \cdot & \cdot & \cdot & 0 \\ 0 & \cdot & & & & \\ \cdot & & \cdot & & & \\ \cdot & & & \cdot & & \\ 0 & & & & & 0 \end{bmatrix}$$

Thus, we obtain

$$\lim_{N \to \infty} C_N |\lambda_1|^{2N} F \begin{bmatrix} 1 & 0 & \cdot & \cdot & \cdot & 0 \\ 0 & \cdot & & & & \\ \cdot & & \cdot & & & \\ \cdot & & & \cdot & & \\ \cdot & & & & \cdot & \\ 0 & & & & & 0 \end{bmatrix} F^{-1} \alpha(0)$$

$$= \lim_{N \to \infty} C_N |\lambda_1|^{2N} (f_1) \begin{bmatrix} \sim T \\ (g_1) \end{bmatrix} \alpha(0) \qquad (6\text{-}15)$$

$$= \lim_{N \to \infty} C_N |\lambda_1|^{2N} (f_1) K$$

where

f_1 is the first column of F

$\underset{(g_1)}{\sim^T}$ is the first row of F^{-1}

K is set equal to $\underset{(g_1)}{\sim^T} \alpha(0)$ in the second equality

From Equation (6-14),

$$1 = \beta^*(N)\,\beta(N) = C_N \left[F\,\Lambda^N\,F^{-1}\,\alpha(0)\right]^* \; C_N \left[F\,\Lambda^N\,F^{-1}\,\alpha(0)\right]$$

By factoring out $|\lambda_1|^{2N}$ and taking the limit as $N \to \infty$, we have, from Equation (6-15),

$$1 = \lim_{N\to\infty} \left[C_N\,|\lambda_1|^{2N}\right]^2 \left[(K)(f_1)\right]^* \left[(K)(f_1)\right]$$

Thus,

$$1 = \lim_{N\to\infty} C_N (\lambda_1)^{2N} \frac{1}{|K|\;|f_1|}$$

and $\beta(N)$ approaches a constant times the first column of F (the largest eigenvector).

The program actually checks the magnitude of the difference between each successive iteration of the eigenvector and stops the iterations when the magnitude becomes sufficiently small. Then, the final iteration is normalized so that $\alpha^* \Omega_{11}\,\alpha = 1$, and the associated eigenvalue is calculated from

$$\Omega_{11}^{-1}\,\Omega_{12}\,\Omega_{22}^{-1}\,\Omega_{21}\,\alpha = |\lambda_1|^2\,\alpha$$

The Γ filter vector, associated with the second group of sensors, is calculated from Equation (6-2) by

$$\Gamma = \lambda \ \Omega_{22}^{-1} \Omega_{21} \alpha$$

where λ is the square root of $|\lambda|^2$. It should be noted that an arbitrary factor of $e^{i\theta}$ is associated with the computation of the filter vector Γ. Since we maximize with respect to $|\lambda|^2$, this arbitrary phasor is to be expected, for it does not change the coherence. This may be considered physically as being equivalent to moving the output point of the MCF system designed to maximize the coherence.

This procedure can be continued to find the successively smaller eigenvalues and their associated eigenvectors.

$$\Omega_{11}^{-1} \Omega_{12} \Omega_{22}^{-1} \Omega_{21} = F \Lambda F^{-1}$$

has the form

$$\sum_{i=1}^{p} |\lambda_i|^2 f_i \tilde{f}_i^T$$

where f_i is the i^{th} eigenvector (the i^{th} column of F) and $\tilde{f}_i^T$ is the i^{th} row of F^{-1}.

Since $F^* \Omega_{11} F = I$, it follows that $F^{-1} = F^* \Omega_{11}$ or $\tilde{f}_i^T = f_i^* \Omega_{11}$. Thus,

$$\Omega_{11}^{-1} \Omega_{12} \Omega_{22}^{-1} \Omega_{21} - |\lambda_1|^2 f_1 f_1^* \Omega_{11} = \sum_{i=2}^{p} f_i |\lambda_i|^2 \tilde{f}_i^T = F \begin{bmatrix} 0 & \cdots & 0 \\ \cdot & |\lambda_2|^2 & \\ \cdot & & \cdot \\ \cdot & & \cdot \\ \cdot & & \cdot \\ 0 & & |\lambda_p|^2 \end{bmatrix} F^{-1}$$

The largest eigenvector of the modified matrix is $|\lambda_2|^2$. The iterative procedure can again be applied to find the second largest eigenvalue and associated eigenvector.

In actual calculations, the crosspower matrix Ω is estimated by direct-transform methods and smoothed.

There has been no attempt to derive the distribution of the estimates of the maximum coherences (the eigenvalues). However, we have made some estimates of the measured group coherence, under the hypothesis that the traces were uncorrelated, by running the program on traces coming from a random noise generator; the results are summarized in Table VI-1. The table shows that a large amount of data is necessary if one wants to maintain a reasonable smoothing interval and have reasonable reliability (stability) in the estimate of the group coherence. Apparently a good rule-of thumb would be to require 10 independent frequency data vectors for each channel.

Table VI-1

GROUP COHERENCES FOR RANDOM NOISE

Number of Traces in Each Partition (1/2 number of total traces)	Time Interval (points) (sec)	Smoothing Interval in Frequency Domain (cps)	Number of Basic Frequency Intervals	Number of Estimates of Group Coherence	Calculated $\|\lambda\|^2$'s
19	4096 pt 409.6 sec	0.2	81	3	0.64, 0.59, 0.64
10	4096 pt 409.6 sec	0.2	81	3	0.36, 0.335, 0.295
10	8192 pt 819.2 sec	0.2	162	1	0.155
10	12288 pt 1228.8 sec	0.2	243	3	0.12, 0.12, 0.135

SECTION VII

GROUP-COHERENCE PROCESSING OF LASA NOISE

Does the noise include any elements which are strongly coherent among subarrays? This is the basic question to be answered by group-coherence processing on the LASA noise.

Used for processing was the 27 April 1966 noise sample which consisted of three 8-min tapes forming a 24-min noise sample with a gap of only a few tenths of a second between tapes. Based on results of the study of group-coherence estimates using random traces (Table VI-1), the amount of data was considered to justify use of about 10 channels only from each subarray while maintaining reasonable resolution (0.2 cps).

Chosen from subarrays A0 and B4 were 10 channels. Sensor locations are shown to scale in Figure VII-1. As a control, 10 channels were selected from subarray F4 and the group coherences were calculated for A0-B4 and A0-F4.

Crosspower matrices are estimated by taking the direct transform of 4096 points from each of three noise tapes (which have been prewhitened), forming the crosspower matrix for each, and smoothing over 81 frequency increments (0.2 cps). Then, the three crosspower matrices are stacked. Additionally, the following are computed for comparison:

- A0-B4 group coherence using only one crosspower matrix and a stack of two of the crosspower matrices just described
- 2-channel coherence from the MCF output of subarrays A0 and B4, which is calculated using 4096 points and a 0.2-cps smoothing interval
- Multiple coherence between seismometer 84, subarray B4, and seismometers 21, 41, 61, 81, 22, 23, 25, 26, 27, 36, 56, and 76 from subarray A0 (the sensors located nearest seismometer 84 of B4), which is calculated from 4096 points of unwhitened data using a smoothing interval of 0.2 cps

Figure VII-2 shows results for the preceding. The following are the salient features of the figure.

- Group coherence for the two subarrays (which are only 9 km apart, center to center) is not extremely high except at very low frequencies (microseism peaks)
- LASA noise is uncorrelated among subarrays above approximately 1 cps
- MCF outputs exhibit considerably less coherence
- No coherence is indicated between A0 and F4 subarrays

Group coherence is very high only at 0.2 cps. This is probably caused by a narrowband directional surface mode.[5] Coherence in the frequency range where the mantle P-wave noise is generally dominant (0.4 to 1.0 cps) falls in the range of 0.3 to 0.7 and is roughly as coherent as the noise from a single point-like source (Section IV).

It is difficult to compare exactly the group coherence with the 2-channel coherences cited in Section IV, for there is some question as to what the sensor spacing should be when one considers group coherence. The group-coherence filters could shut off all except the nearest two sensors and thus be equivalent to a 2-channel coherence but much more closely spaced than the subarray centers. An examination of the filter responses indicates that this did not happen. However, it is difficult to estimate how much effect subarray-element spacing should have when comparing the 2-channel coherences with the group coherences.

Wavenumber responses of the two filter systems (for A0 and B4) have been computed, but no useful interpretation of them can be made so they are not presented.

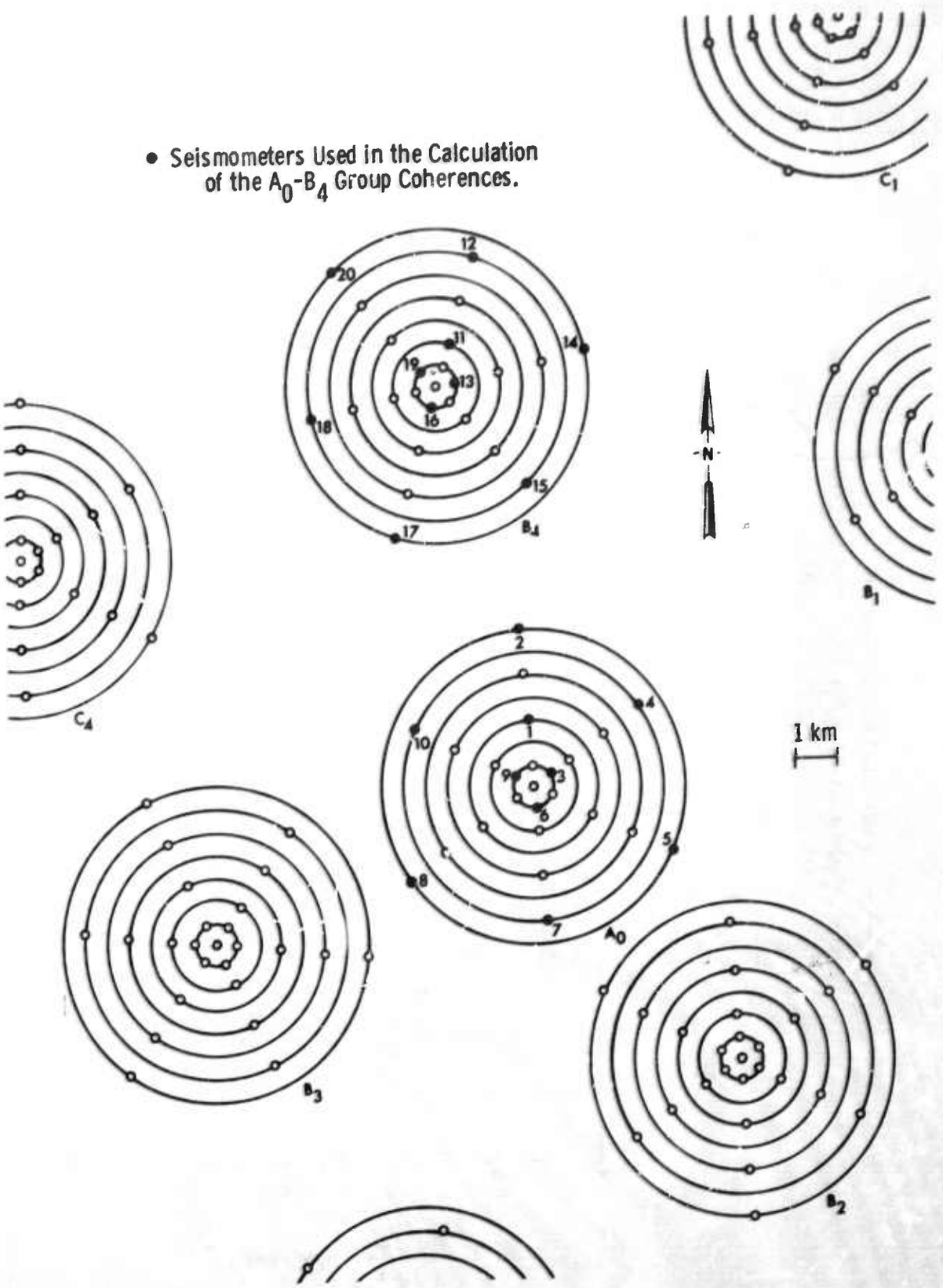

Figure VII-1. Layout of Central Portion of LASA

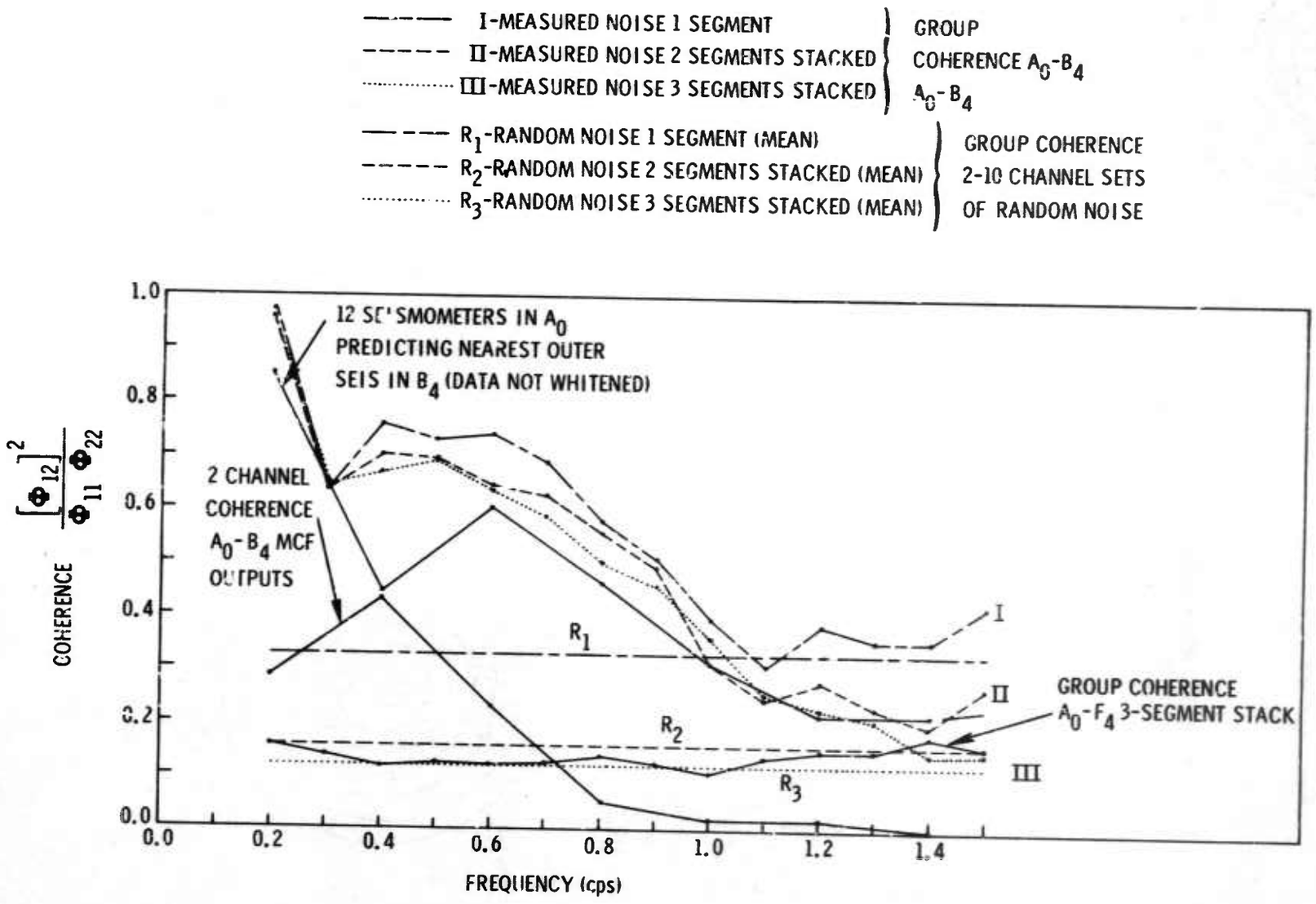

Figure VII-2. Group Coherences of LASA Noise

LASA noise is apparently incoherent among subarrays above approximately 1 cps. Group coherence above 1.0 cps agrees well with the values computed from the random noise; this is about the same frequency where the noise appears incoherent within a subarray.[5,6]

The MCF processor gives an output which shows considerably less 2-channel coherence than that of the group-coherence filters, but this is to be expected. The group-coherence filter systems should "latch on" to elements of the noise field which are most similar between the two subarrays and should try to reject the remainder.

Additionally, the group coherence is greater than the multiple coherence between the outermost element of the B4 array and the 12 closest elements from subarray A0. This suggests that there is some coherence gain by rejection of part of the less coherent noise.

Group coherence for the A0-F4 subarrays stays very near the level expected for uncorrelated traces. There could be some coherence among these subarrays, however, which would not be seen due to the smoothing involved in the estimate of the crosspower matrix. These subarrays are so widely separated that even a perfectly coherent plane wave would show no coherence unless the apparent velocity between the two arrays were very high (Section II).

The A0-F4 group coherence has significance only as a control to indicate that the calculation of the group coherence is behaving in a reasonable manner.

A large signal has been processed as a check of group coherence. Group coherence is calculated between subarrays B2 and C2 for a signal from Andreanof Islands (51.4°N, 179.7°W, Δ = 46.5°, Az = 304.1°, recorded on 23 November 1965). From the LASA site, this would give a Δ of 46.5° and an azimuth of 304°. The apparent horizontal velocity of the P wave would be 14.3 km/sec. The event was large (mag 5.6), complex, and well-recorded at LASA.

Group coherence is calculated using 13 sensors from each subarray (10, 3rd ring, 5th ring, 7th ring, and 8th ring). Figure VII-3 shows some representative traces of the event. Group coherence is calculated at 1.0 cps using 3900 points with a 0.2-cps smoothing interval. To stabilize the inversion problem, 5-percent random noise is added to the crosspower matrix.

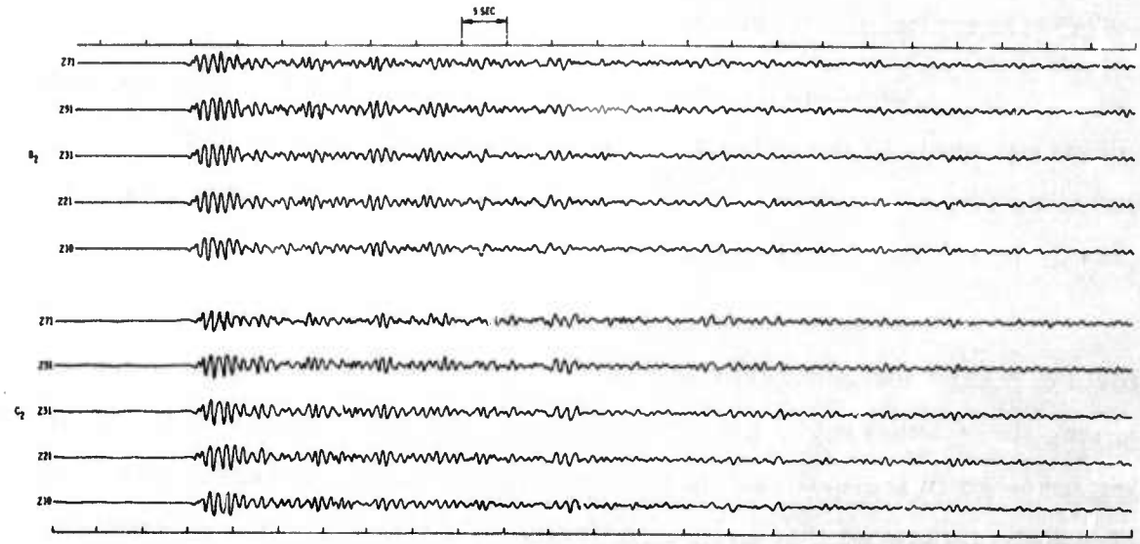

Figure VII-3. Andreanof Islands Earthquake

The calculated group coherence at 1 cps is 0.96. A pair of exactly similar traces time-shifted appropriately and processed as above (same smoothing and random-noise addition) would have a 2-channel coherence of approximately 0.82. Recall that 26 total channels have been used to produce the output which gives the 0.96 coherence estimate; this means that the traces can be used to reduce random noise. Also, there are approximately two degrees of freedom per filter point, which suggests a biased high estimate of the group coherence.

Figuve VII-4 shows the wavenumber response of the group-coherence filters for subarrays A0 and B4. The earthquake signal's location is shown by a cross in each plot. These plots indicate that the group-coherence filter systems pass the P-wave energy, which would be expected to be the most coherence element. The group-coherence filters have indicated, in this simple case, the location (in f-$\vec{k}$ space) of the most coherent element of the data.

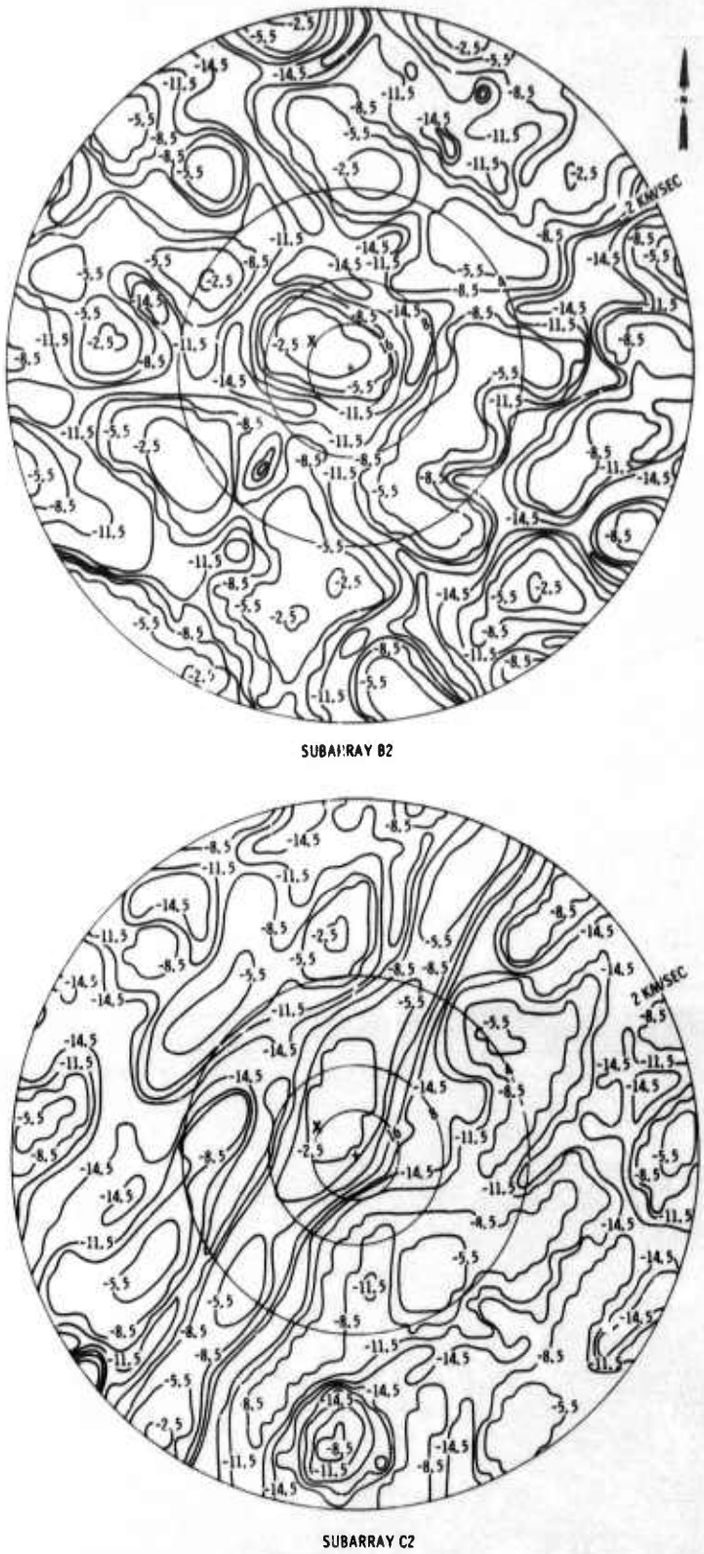

Figure VII-4. Responses of Group-Coherence MCF Systems at 1.0 cps

SECTION VIII
LASA COHERENCE

The subarray outputs at LASA are, in general, essentially incoherent except within the B ring of subarrays; even here, the coherence is generally 0.5 or less except at the microseism peak. This indicates that there can be no important gain from coherence processing of subarray outputs.

Processing designed to maximize the coherence between two subarrays 9 km apart tends to indicate that the P-wave noise contains some moderately coherent elements. This experiment used insufficient data to be truly definitive, however.

The observed coherence among subarrays could be strongly influenced by

- The geometry of the large array. (The filling of the "unit cell" in f-$\vec{k}$ space by the seismic energy destroys coherence)
- Distortion of plane-wave seismic energy by local inhomogeneities in the crust or upper mantle (which results in a smearing-out of energy in wavenumber and reduced coherence)
- Subarray processing which could possibly reduce P-wave coherence
- Coherence estimates which tend to be biased on the low side

LASA has no true unit cell in f-$\vec{k}$ space due to nonuniform spacing, but the effect is qualititively the same as that of an equally spaced array. The model studies (Section VI) indicate that good, fairly broadband coherence can be expected out through the D ring when the P-wave noise is strongly dominated by point-like sources. If the P-wave noise were isotropic, one would expect to find essentially no coherence above the microseism peak for the LASA spacing.

The "random" noise component has been observed to increase (in percentage of total) with frequency within subarray dimensions.[5] This is probably the result of the smearing-out of plane waves by local inhomogeneities in the crust or upper mantle. These effects become increasingly severe as the wavelengths decrease (increasing frequency).

Such differences are represented on a larger scale by the travel-time anomalies observed over the LASA aperture. These large travel-time anomalies strongly suggest that the coherence of the noise (unless it were a point source) would be severely reduced by local inhomogeneities in the crust or upper mantle under LASA.

There is strong evidence at TFO[7] that the P-wave noise is (sometimes, at least) strongly dominated by somewhat point-like sources such as those used in the model studies (Sections IV and V). However, no coherences of the order expected from such a model were observed in the LASA noise, again suggesting that local variations in crust or upper mantle affect measured coherence.

There is relatively little information upon which to assess the effects of the subarray processing on coherence. However, for the one case where prediction among subarrays was made with a single seismometer, with summation of subarray elements, and with an isotropic multichannel filter system (Section V), the summation and MCF outputs gave very similar results and the single seismometers gave noticeably poorer prediction results. By no means is this a definitive experiment, but it tends to suggest that the subarray processing does not severely reduce the P-wave coherence.

The group coherence, however, was considerably higher than the comparable 2-channel coherence for the 27 April noise sample (Section V). One possible explanation (of several) for this is that the subarray processing is destroying useful P-wave noise coherence.

Data available to date are insufficient to state conclusively whether subarray processing is destroying useful P-wave coherence.

The biasing effect of smoothing on coherence has already been discussed. Coherence estimation is made difficult by the degree of smoothing needed. A small amount of smoothing reduces bias and prevents the overlapping of noise modes; a large amount of smoothing gives reliability to the estimates. This has been a particular handicap to group-coherence processing where a large number of sensors are desirable and available (25 from each of 2 subarrays). A noise sample sufficiently long for good estimates of the most coherent elements between two moderately separated subarrays (e.g., A0 and the D ring) is desirable. This would require approximately 10 hr of data if the analysis were to include surface-mode energy, or about 4 hr of data if one were interested only in P-wave noise.

One reason for lack of coherence over larger distances (lateral inhomogeneities in the crust and upper mantle) may be a function of location. The Montana LASA is located on a thick section of Cretaceous and Tertiary shales. Douze[8] has suggested that ambient noise is less interpretable at sites where thick shale sections exist. A large array in a shield area could possibly exhibit better P-wave coherence than does the LASA.

SECTION IX

REFERENCES

1. Koopmans, L. H., 1964, On the multivariate analysis of weakly stationary stochastic processes: Annals of Mathematical Statistics, v. 35, n. 4, Dec.

2. Anderson, T. W., 1958: An Introduction to Multivariate-Statistical Analysis, John Wiley & Sons Inc., New York.

3. Goodman, N. R., 1963, Statistical analysis based on a certain multivariate complex Gaussian distribution (an introduction): Annals of Mathematical Statistics, v. 34, n. 1, Mar.

4. Burg, J. P., Texas Instruments Incorporated (unpublished): Statistical Properties of Multichannel Noise Prediction Filters.

5. Texas Instruments Incorporated, 1967 (to be published): Analysis of Subarray Wavenumber Spectra, LASA Spec. Rpt. No. 6, Contract AF 33(657)-16678.

6. Texas Instruments Incorporated, 1967 (to be published): Subarray Processing, LASA Spec. Rpt. No. 3, Contract AF 33(656)-16678.

7. Texas Instruments Incorporated, 1967: Analysis of K-Line Wavenumber Spectra from the TFO Long-Noise Sample, Array Research Spec. Rpt. No. 23, Contract AF 33(657)-12747, 28 Feb.

8. Douze, E. J., 1967, Short-period seismic noise: Bull. Seis. Soc. Am., n. 57, n. 1, Feb., p. 55-81.

UNCLASSIFIED

Security Classification

DOCUMENT CONTROL DATA - R&D

(Security classification of title, body of abstract and indexing annotation must be entered when the overall report is classified)

1. ORIGINATING ACTIVITY (Corporate author)
Texas Instruments Incorporated
Science Services Division
P. O. Box 5621, Dallas, Texas 75222

2a. REPORT SECURITY CLASSIFICATION
Unclassified

2b. GROUP

3. REPORT TITLE
LARGE-ARRAY SIGNAL AND NOISE ANALYSIS – SPECIAL SCIENTIFIC REPORT NO. 13 – SHORT-PERIOD NOISE COHERENCE AMONG SUBARRAYS

4. DESCRIPTIVE NOTES (Type of report and inclusive dates)
Special Scientific

5. AUTHOR(S) (Last name, first name, initial)
Binder, Frank H.

6. REPORT DATE	7a. TOTAL NO. OF PAGES	7b. NO. OF REFS
20 October 1967	75	8

8a. CONTRACT OR GRANT NO.	9a. ORIGINATOR'S REPORT NUMBER(S)
Contract No. AF 33(657)-16678	
b. PROJECT NO.	
c. AFTAC Project No. VT/6707	9b. OTHER REPORT NO(S) (Any other numbers that may be assigned this report)
d.	

10. AVAILABILITY/LIMITATION NOTICES
This document is subject to special export controls and each transmittal to foreign governments or foreign nationals may be made only with prior approval of Chief, AFTAC.

11. SUPPLEMENTARY NOTES	12. SPONSORING MILITARY ACTIVITY
ARPA Order No. 599	Air Force Technical Applications Center VELA Seismological Center Headquarters, USAF, Washington, D.C.

13. ABSTRACT

Much of the analysis of the mantle P-wave noise proposed for this contract depended on the ability to perform coherent processing by treating seismic noise as a compilation of plane waves using the large aperture available at LASA. The subarray outputs should be P-wave-limited, and the large array could be used to dissect the P-wave noise; therefore, it is extremely important to understand the coherence of the subarray outputs.

This report presents the results of coherence studies among subarrays. Principal results of the study include the development of a program to compute multiple coherences and thus estimate multichannel coherence. A new processing technique to design filters that maximize the coherence between the output of two groups of sensors (group coherence) was developed and programed. Presented are results of measured 2-channel and multiple coherence, indicating that the subarray outputs generally are moderately coherent below about 1 cps only within the B ring of the subarrays. Also presented are 2-channel and multiple coherences for several possible noise models. A study of these coherences suggests that the most reasonable models would give little coherence between A0 and the E and F rings. Comparison of model-study results with measured coherences suggests that a considerable portion (25 percent or more) of the subarray output power is not interpretable as seismic energy.

DD FORM 1 JAN 64 1473

UNCLASSIFIED

Security Classification

14 KEY WORDS	LINK A		LINK B		LINK C	
	ROLE	WT	ROLE	WT	ROLE	WT
Large-Array Signal and Noise Analysis Noise Coherence Among Subarrays Multiple-Coherence Program 2-Channel Coherences Multichannel Coherence Group Coherence						

INSTRUCTIONS

1. ORIGINATING ACTIVITY: Enter the name and address of the contractor, subcontractor, grantee, Department of Defense activity or other organization *(corporate author)* issuing the report.

2a. REPORT SECURITY CLASSIFICATION: Enter the overall security classification of the report. Indicate whether "Restricted Data" is included. Marking is to be in accordance with appropriate security regulations.

2b. GROUP: Automatic downgrading is specified in DoD Directive 5200.10 and Armed Forces Industrial Manual. Enter the group number. Also, when applicable, show that optional markings have been used for Group 3 and Group 4 as authorized.

3. REPORT TITLE: Enter the complete report title in all capital letters. Titles in all cases should be unclassified. If a meaningful title cannot be selected without classification, show title classification in all capitals in parenthesis immediately following the title.

4. DESCRIPTIVE NOTES: If appropriate, enter the type of report, e.g., interim, progress, summary, annual, or final. Give the inclusive dates when a specific reporting period is covered.

5. AUTHOR(S): Enter the name(s) of author(s) as shown on or in the report. Enter last name, first name, middle initial. If military, show rank and branch of service. The name of the principal author is an absolute minimum requirement.

6. REPORT DATE: Enter the date of the report as day, month, year, or month, year. If more than one date appears on the report, use date of publication.

7a. TOTAL NUMBER OF PAGES: The total page count should follow normal pagination procedures, i.e., enter the number of pages containing information.

7b. NUMBER OF REFERENCES: Enter the total number of references cited in the report.

8a. CONTRACT OR GRANT NUMBER: If appropriate, enter the applicable number of the contract or grant under which the report was written.

8b, 8c, & 8d. PROJECT NUMBER: Enter the appropriate military department identification, such as project number, subproject number, system numbers, task number, etc.

9a. ORIGINATOR'S REPORT NUMBER(S): Enter the official report number by which the document will be identified and controlled by the originating activity. This number must be unique to this report.

9b. OTHER REPORT NUMBER(S): If the report has been assigned any other report numbers *(either by the originator or by the sponsor)*, also enter this number(s).

10. AVAILABILITY/LIMITATION NOTICES: Enter any limitations on further dissemination of the report, other than those imposed by security classification, using standard statements such as:

(1) "Qualified requesters may obtain copies of this report from DDC."

(2) "Foreign announcement and dissemination of this report by DDC is not authorized."

(3) "U. S. Government agencies may obtain copies of this report directly from DDC. Other qualified DDC users shall request through _____."

(4) "U. S. military agencies may obtain copies of this report directly from DDC. Other qualified users shall request through _____."

(5) "All distribution of this report is controlled. Qualified DDC users shall request through _____."

If the report has been furnished to the Office of Technical Services, Department of Commerce, for sale to the public, indicate this fact and enter the price, if known.

11. SUPPLEMENTARY NOTES: Use for additional explanatory notes.

12. SPONSORING MILITARY ACTIVITY: Enter the name of the departmental project office or laboratory sponsoring *(paying for)* the research and development. Include address.

13. ABSTRACT: Enter an abstract giving a brief and factual summary of the document indicative of the report, even though it may also appear elsewhere in the body of the technical report. If additional space is required, a continuation sheet shall be attached.

It is highly desirable that the abstract of classified reports be unclassified. Each paragraph of the abstract shall end with an indication of the military security classification of the information in the paragraph, represented as *(TS)*, *(S)*, *(C)*, or *(U)*.

There is no limitation on the length of the abstract. However, the suggested length is from 150 to 225 words.

14. KEY WORDS: Key words are technically meaningful terms or short phrases that characterize a report and may be used as index entries for cataloging the report. Key words must be selected so that no security classification is required. Identifiers, such as equipment model designation, trade name, military project code name, geographic location, may be used as key words but will be followed by an indication of technical context. The assignment of links, rules, and weights is optional.